Master's thesis

NTNU
Norwegian University of Science and Technology
Department of Energy and Process Engineering

Amanda Malene Eide Buan

# Analysis of ground-source heat pump and hybrid PVT for Norwegian conditions

Master's thesis in Energy and Environment
Supervisor: Laurent Georges
Co-supervisor: Mohammad Liravi
June 2023

NTNU
Norwegian University of Science and Technology

Amanda Malene Eide Buan

# Analysis of ground-source heat pump and hybrid PVT for Norwegian conditions

Master's thesis in Energy and Environment
Supervisor: Laurent Georges
Co-supervisor: Mohammad Liravi
June 2023

Norwegian University of Science and Technology
Department of Energy and Process Engineering

NTNU
Norwegian University of
Science and Technology

**Page intentionally left blank**

# Problem description

Heat pump is an energy efficient technology for the heating and cooling of buildings. Different heat sources can be used, such as the outdoor air or the ground. Solar energy can complement the heat pump. In particular, hybrid photovoltaic thermal collectors (PVT) produce electricity and heat at low temperature. Firstly, the water flow cools down the photovoltaic cells leading to an increase of their conversion efficiency. Secondly, the heat can be used as a source for the heat pump while the electricity produced can drive its compressor. This combination PVT + heat pump is currently investigated within the ChinoZEN projects where Chinese and Norwegian research institutions collaborate. However, both contexts are different. While solar energy is available during wintertime for lower latitude in China, solar irradiation is limited in Scandinavia during the heating season. In addition, China typically uses high temperatures for space heating while Norway promotes low supply water temperature. Therefore, the potential of combined PVT + heat pump is different in both conditions. The project aims at analyzing this potential for high latitude and/or cold climate using PVT in combination with borehole seasonal thermal energy storage (BTES). The analysis will be the continuation and improvement of the ongoing research in our group. The system performance will be then evaluated using thermal dynamic simulations (most probably in TRNSYS and/or IDA ICE).

Assignment given: 16th of January 2023

Supervisor: Laurent Georges, EPT

Co-supervisor: Mohammad Liravi, EPT

# Abstract

The objective of this work has been to perform an analysis of a GSHP with PVT in TRNSYS. The system was to be analyzed with regards to energy efficiency, but also from an economical perspective, compared to a GSHP with and without PV panels. A relatively large focus has been on the thermal behavior of the BHs.

The three following simulation models have been used:

- Model 1: GSHP
- Model 2: GSHP with PVT
- Model 3: PV

The models have been simulated with a variation of number of BHs and areas of the PVT collector and the PV panels. The effect of reducing the BH spacing from 20 m to 10 m with PVT has been investigated, as well as the effect of increasing the power coverage of the GSHP. Lastly, an economical analysis has been performed to investigate if the system with PVT and less BHs is economically viable, compared to a conventionally sized BHE field.

The results showed that an undersized BHE field will lead to a steeper decrease in both the temperature of the BHs and the system's performance over the years. Introducing PVT has shown to increase the performance and the average brine temperature of the GSHP system. A reduction of 4 BHs in the system with PVT was compared to a normal sized GSHP system. The results did not favor reducing the number of BHs with PVT, as the energy savings were not sufficient enough to justify the investment cost, compared to a stand-alone GSHP with more BHs. The most promising option based on the performance is a traditionally sized BHE field with PVT. Further, the work showed that increasing the PVT area did not reduce the auxiliary heating for SH markedly, but it did increase the average temperature of the BHs.

In the economical assessment, all three systems investigated were accepted according to the criteria of the pay-back period, with the GSHP having the shortest one. A traditionally sized GSHP with PV has shown to have the lowest annual total cost, and would be the desirable option if land area is not limited.

# Sammendrag

Formålet med dette arbeidet har vært å utføre en analyse av en grunnvarmepumpe med PVT-paneler i TRNSYS. Systemet skulle analyseres både med tanke på energieffektivitet, men også fra et økonomisk perspektiv, sammenlignet med en grunnvarmepumpe med og uten solceller. Et relativt stort fokus har vært på den termiske oppførselen til energibrønnene.

Tre simuleringsmodeller har blitt brukt:

- Model 1: Grunnvarmepumpe
- Model 2: Grunnvarmepumpe med PVT-paneler
- Model 3: Solceller

Modellene har blitt simulert med en rekke antall energibrønner og ulike arealer av PVT- og solcellepaneler. Effekten av å redusere avstanden mellom brønnene fra 20 m til 10 m med PVT-paneler har blitt undersøkt, så vel som å øke effektdekningsgraden til varmepumpen. I tillegg, har en økonomisk analyse blitt gjennomført for å undersøke om et system med PVT og færre energibrønner er økonomisk levedyktig, sammenlignet med et borrefelt av tradisjonell størrelse.

Resultatene viste at et underdimensjonert borrefelt fører til en raskere nedgang i både gjennomsnittlig temperatur i brønnene og systemytelse over tid. Å introdusere PVT-paneler har vist å øke ytelsen og gjennomsnittlig temperatur av brønnvæsken til varmepumpesystemet. En reduksjon på 4 brønner av systemet med PVT ble sammenlignet med en tradisjonell grunnvarmepumpe. Resultatene var ikke i favør med å redusere antall brønner ved bruk av PVT, da energisparingene ikke er tilstrekkelig til å dekke investeringskostnaden, sammenlignet med en enkeltstående grunnvarmepumpe med flere borrehull. Den mest lovende løsningen basert på ytelsen, er en grunnvarmepumpe med et normalt antall energibrønner og PVT. Videre, viste arbeidet at å øke arealet med PVT-panel ikke minket tilleggsvarmen til romoppvarming markant, men det økte derimot gjennomsnittstemperaturen i borrehullene.

I den økonomiske analysen ble alle tre systemene godkjent i henhold til inntjeningsmetodens kriterier, hvor grunnvarmepumpen hadde den korteste perioden. En vanlig dimensjonert grunnvarmepumpe med solceller hadde den laveste årskostnaden, og vil være det mest ønskelige valget dersom tilgjenelig landområde ikke er en begrensning.

# Preface

This report is the written work of my master thesis at the Norwegian University of Science and Technology (NTNU), at the department of energy and process engineering. The work was performed and written during the spring of 2023. The thesis accounts for 30 credits of the master degree in the study program Energy and Environment at NTNU. The title of the master thesis is "Analysis of ground-source heat pump and hybrid PVT for Norwegian conditions", and it is a continuation of the specialization project with the same title.

This work has given me a deeper understanding of ground-source heat pump systems combined with solar technology. During the work I have faced difficulties with understanding why the systems are behaving as they are. It has been an educational journey and I have gained insight into geothermal storage and solar thermal energy. I have also gained valuable insight into the simulation tool TRNSYS.

Firstly, I would like to thank my supervisor, Associate Professor Laurent Georges, for all the guidance and excellent constructive feedback I have gotten through this work. I would also like to thank my co-supervisor, PhD student Mohammad Liravi, for all the help and feedback I have gotten.

Trondheim, June 11, 2023

Amanda M.E. Buan

Amanda Malene Eide Buan

# Contents

# Abbreviations

**PV** Photovoltaic

**PVT** Photovoltaic-Thermal

**ST** Solar Thermal Collector

**FPC** Flat Plate Collector

**ETC** Evacuated Tube Collector

**UTES** Underground Thermal Energy Storage

**HP** Heat Pump

**GSHP** Ground-Source Heat Pump

**SAGSHP** Solar Assisted Ground-Source Heat Pump

**HX** Heat Exchanger

**BTES** Borehole Thermal Energy Storage

**BHE** Borehole Heat Exchanger

**FPC** Flat-Plate Collector

**SAHP** Solar-Assisted Heat Pump

**PVT-SAHP** Photovoltaic-Thermal Solar-Assisted Heat Pump

**BPS** Building Performance Simulation

**COP** Coefficient Of Performance

**SPF** Seasonal Performance Factor

**$CO_2$** Carbon Dioxide

**DHW** Domestic Hot Water

**IDA-ICE** IDA Indoor Climate and Energy

**TRNSYS** Transient System Simulation Tool

**TESS** Thermal Energy System Specialists

**SH** Space Heating

| | |
|---|---|
| **kWh** | Kilo Watt Hour |
| **kWp** | Kilo Watt Peak |
| **kW** | Kilo Watt |
| **m** | Meter |
| **K** | Kelvin |
| **NS** | Norwegian Standard |
| **TMY** | Typical Meteorological Year |
| **DOT** | Design Outdoor Temperature |
| $N_{col}$ | Number of collectors |
| $A_{col}$ | Collector area |

# List of Figures

# List of Tables

# 1 Introduction

Buildings are a relatively large consumer of energy. In 2017, the energy use for housing in Norway was 47.6 TWh, which corresponds to 22% of the total use [1]. The use is mainly for heating, such as space heating and heating of domestic hot water, but also technical equipment and lighting.

The main energy source in Norway is electricity, followed by biofuels [1]. The share of electricity is 83%, and it is continuously rising due to more electric appliances and the phasing out of fossil fuels for space heating. More and more electrical vehicles will also contribute to increase the electricity consumption, as well as a less fuel dependent future in other sectors.

A heat pump (HP) is an effective way of heating that reduces the energy consumption markedly. The use of HPs in Norway has rapidly increased the last few years, and in 2016 more than 900 000 units were installed in total [2]. Air-to-air HPs are dominating, but the use of ground-source HP (GSHP) has grown as well.

A downside of the popular air-sourced HP is that when the heating demand is at its highest during the winter in cold climates, its performance is at its lowest. A GSHP on the other hand, provides a more stable performance throughout the year. The downside with the GSHP for larger buildings, especially in dense urban areas, is that the borehole (BH) field takes up a lot of space. Additionally, it can be undersized which can lead to cold boreholes and a reduced efficiency with time.

The past year, there has been a growing interest in solar-assisted GSHP, especially photovoltaic-thermal collectors. In this manner, the BHs can be recharged with solar heat and the amount of imported energy is reduced. Storing the solar heat creates a borehole thermal energy storage (BTES).

## 1.1 Objective

The objective of this thesis has been to analyze the performance of a GSHP with PVT in TRNSYS, compared to a stand-alone GSHP and a GSHP with PV. The main focus has been on energy efficiency, but also if adding PVT can reduce the BHE field and the cost of the system. In addition, there is a lack of documentation of GSHP systems with PVT in high latitudes in the literature and few existing projects to make measurements from.

## 1.2 Delimitations

The cooling load in Norway is very small and has thus been neglected. Pipes and losses from distribution of DHW and the legionella circuit have not been included in the models. This is however done in all the models, so the results are still comparable. However, it could affect the results when reducing the BHE field.

A simple economical analysis has been performed. The surplus of produced electricity on-site is assumed exported and sold with the yearly average electricity price. In addition, the PV efficiency of the PVT is lower than the efficiency of the PV panel.

# 2 Background and methodology

This section contains relevant theory and information about the technologies applied in this thesis, in addition to a review of performance in colder climates and a state-of-the-art. Since this is a continuation of the specialization project [3] performed the fall of 2022, the background section contains parts from the project that has been elaborated.

## 2.1 The Norwegian building stock

The distribution of different building typologies in the Norwegian building stock can be found in table 2.1. Most dwellings in Norway are single-family houses, but the energy systems in apartment blocks are typically more complex and will thus be the focus in this section.

| Building typology | Share of dwellings |
|---|---|
| Single-family house | 48% |
| Terraced house | 21% |
| Apartment block | 25 % |
| Other types | 5 % |

Table 2.1: Distribution of building types in the Norwegian building stock [4].

In 2016, the Norwegian government adopted a political objective to reduce the energy use from existing buildings by 10 TWh by 2030 [5]. To reach this goal, energy requirements alone is not enough, as it only flattens out the increase in energy consumption, but measures such as installation of heat pump units and production of renewable energy on-site are needed.

The recent years, the energy requirements for new buildings have become more and more strict to reduce the energy consumption from the building sector. A large part of the building stock is built before the requirements became strict enough to reduce the energy demand noticeably. Enova's building statistics [6] states that the average apartment block is built in 1989 and has a specific energy demand of 143 kWh/m$^2$. The same report also says that the main energy sources for apartment blocks are electricity and district heating. This based on data reported from only 40 apartment blocks. A better illustration of the distribution of the construction years can be found in figure 2.1.

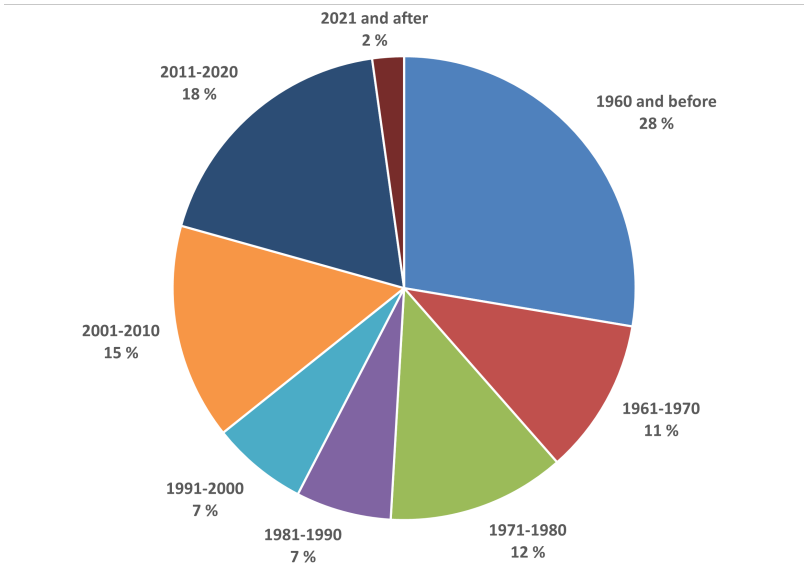


Figure 2.1: Construction year for apartment blocks in Norway [7].

### 2.1.1 TABULA and TABULA WebTool

TABULA was a study performed by the Intelligent Energy Europe (IEE) from 2009-2012. The goal was to gather information of the national building typologies for European countries to represent the building stock of the nationalities. The typologies includes, among other, classification of existing typologies according to age, size and other parameters, and example buildings with typical energy consumption [3].

The study TABULA was the starting point of the project EPISCOPE, which has later been further expanded. The objective of EPISCOPE was to take the refurbishment processes of the existing building stock more effective. The TABULA WebTool was developed as a part of the projects EPISCOPE and TABULA, and is a way to access the information gathered in the projects. The WebTool provides calculations of all of the exemplary buildings with energy demands and potential energy savings that can be achieved by different degrees of refurbishments [3].

## 2.2 Electricity prices

In Norway, 90% of all electricity comes from hydro-power plants. The low operating and start/stop costs associated with hydro-power leads to cheaper electricity, compared to other energy sources. This has for several years made high-quality energy

like electricity the main energy source for heating. [3]

The average electricity price in 2022 was record high at 2.35 NOK/kWh (ca. 0.2 EUR/kWh) [8], including energy price, network rent and taxes. This is 66% higher than the year before, which also was a year with an unusual high electricity price. After electricity financial aids from the authorities, the average price was reduced to 1.44 NOK/kWh (ca. 0.12 EUR/kWh).

The downside of solar energy production is that the production is at its highest when the consumption is at its lowest. A possibility is to export the surplus electricity back to the grid. Some electricity suppliers [9] offers this possibility with Nord Pool's spot price.

## 2.3 Potential of solar energy

In Norway, PV panels are typically used in places where there is no connection to the grid, like for cabins [10], and the production from PVs in Norway are 0.23 $TWh/year$ [11]. This corresponds to one thousandth of the total energy generation. The solar radiation on a horizontal surface ranges from 700 to 1100 kWh/m$^2$, and a facility with 1 kWp will typically produce 800-900 kWh/year [10]. With a tilted surface, the solar radiation and the possibility of utilizing the solar energy is slightly increased. The optimal slope of the surface is related to the latitude and when it is desired to have maximal production. With a steeper slope, the production when the sun has a low position in the sky, like in the fall and spring, is increased.

## 2.4 Solar thermal collectors

Solar thermal collectors (ST) are a simple way of collecting and utilizing the solar heat for households. It converts energy from solar radiation to internal energy for a heat carrier, like water or air. The fluid then transports the heat to a storage tank, SH-equipment or underground thermal energy storage [3].

The design of the ST collector can be divided into two variants: non-concentrating and concentrating. For the non-concentrating type, the absorber surface is approximately the same as the overall collector area [3]. Flat plate collectors (FPC) and evacuated tube collectors (ETC) are both examples of this type of collectors, and they are mainly designed for applications requiring energy delivery at temperatures of 60-250°C [12].

The concentrating collectors have a large area of reflectors or mirrors that redirect

the sun-rays to a smaller absorber [3]. Collectors of this type provides heat at a much higher temperature than the non-concentrating ones, at about 400-1000 °C [12]. Due to this, the focus further on in this section will be on FPC and ETC.

### 2.4.1 Flat plate collectors

The flat-plate collectors (FPC) makes use of both direct and diffuse radiation, and are suitable for low-temperature applications, namely heating of DHW and SH purposes. They are commonly used due to their low investment and operation cost [3]. The FPC is typically used in building applications where the temperatures does not exceed 80 °C [13]. The FPC usually consists of the following components: absorber plate, insulation, flow passages and casing. The collectors can be glazed or unglazed, where the unglazed ones are characterized by an absorber without a glass or translucent plastic cover. Because of this, the heat loss from it is larger and they are typically used for low temperature applications with a requested temperature lower than 30 °C, such as heating swimming pools [14]. An illustration of the collector can be found in figure 2.2.

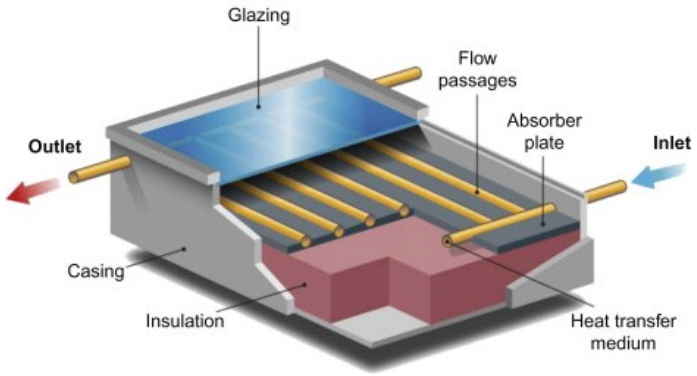


Figure 2.2: Schematic illustration of a glazed FPC [13].

### 2.4.2 Evacuated tube collectors

The evacuated tube collectors (ETC), like FPC, collects both direct and diffuse radiation. They usually consists of parallel rows of glass tubes with each tube containing a heat pipe, where the air between the tubes has been removed to form a vacuum [13]. In this manner, the convective and conductive heat losses are reduced, due to vacuum having a higher insulation property. A schematic of the ETC can be seen in figure 2.3.

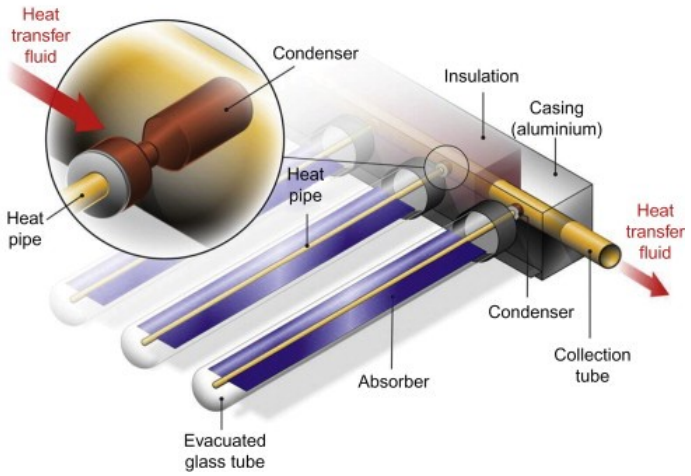


Figure 2.3: Schematic illustration of an ETC with heat pipes [13].

The ETCs are commonly used for preparation of DHW and SH in residential and commercial buildings. They typically have efficiencies of 30-45%, and usually outperforms the FPCs in colder climates as the temperature is less affected by the surrounding temperature [13].

S. Mohasseb and A. Kasaeian [15] compared the performance of the FPC and ETC for building applications in warm and cold climates in TRNSYS. The results showed an advantage for the ETC in a cold climate, whereas the performance was similar for both in warmer climates. The performance of the FPC was also found to be more affected by the environmental conditions than the ETC.

### 2.4.3 Economy and lifetime

The FPC is the most common used in Norway due to its robustness when it comes to rough weather. The price is typically from 6 000 NOK and up [16]. An ETC gives a better efficiency but is less suited to the Norwegian climate. The price typically ranges from 10 000 - 30 000 NOK. The lifespan is usually around 20 to 30 years [17] for ST collectors, depending on the type.

## 2.5 Photovoltaic panel

The PV panel uses the photon energy of the solar rays to generate electricity. Even though the performance of the PV has ascended the past decades, from 1% in 1941

to above 20% the past decades, there are some parameters that occurs in operating condition that directly affects the performance of the PV. One of these parameters is the surface temperature. High temperature from continuous exposure to solar radiation leads to a reduced open circuit voltage ($V_{OC}$). Which, as can be seen in equation 2.1, has a negative impact on the PV panel's efficiency[3]. The production from a PV facility in Norway is typically 650-1000 kWh/kWp [11].

$$\eta = \frac{V_{OC} \cdot I_{SC} \cdot FF}{P_{in}} \tag{2.1}$$

### 2.5.1 Economy and lifetime

Communication with Gilbert Jensen in Carbon Neutral Energy on the 18th of April 2023 gave some indication of prices for PV:

Facilities over 30 kWp:

1. PV: 900 - 1 200 EUR/kWp

Facilities less than 30 kWp:

1. PV: 1 000 - 1 500 EUR/kWp

These prices are excluded VAT, and refers to both material and installation per installed kWp.

## 2.6 Photovoltaic-thermal collectors

A PVT collector is a combination of a PV panel and a solar thermal collector, and generates both electricity and heat in the same module. The generation of heat cools down the PV panel, which leads to an increase in the efficiency of electricity production[3]. The heat extraction from the PV can increase the generation by 10-15% per year [18], compared to conventional PV panels. The idea of combining the PV panel and ST collector is not a new idea. As early as in 1973, professor Böer built a house called 'Solar One' that was equipped with a PV hybrid collector. The interest in the product has however been limited until recent years [3].

Similar to the ST collector, the PVT module can be glazed or unglazed. The glazed PVT will produce more thermal energy and have a higher output temperature, but this yields a lower electrical production than a stand-alone PV. The unglazed PVT will have a higher electrical production, than both the glazed PVT and conventional

PV, but a lower thermal performance [19]. The PVT can also be insulated or uninsulated. The insulated version is usually used in high-temperature applications, such as pool heating or preheating of DHW. For low-temperature systems, for instance with a brine-water HP, the unsinsulated type is typically used.

The cells in the PVT is the same as conventional PV panels, but there are several solutions for the thermal absorber part. The absorber is an important factor to the performance of the PVT, particularly liquid-type PVT, as the heat transfer from the PV to the thermal medium depends on it. The PVT can be divided into two types, depending on the absorber: sheet-and-tube absorber (figure 2.4a) and fully wetted absorber (figure 2.4b). The latter increases the heat transfer surface and is thus believed to have a better thermal performance [20].

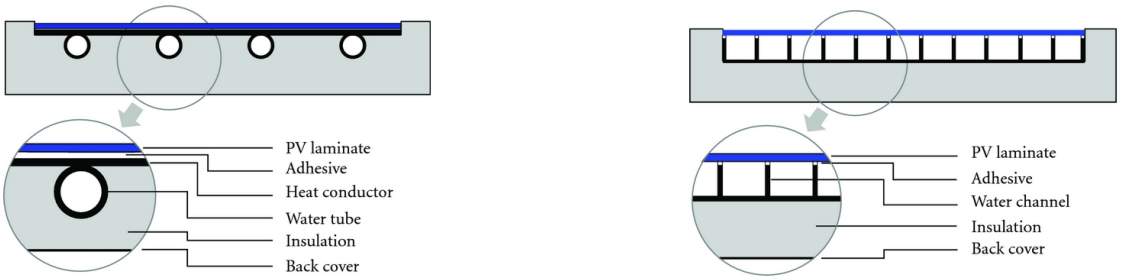


(a) Schematic of a sheet-and-tube PVT [20].

(b) Schematic of a fully wetted PVT [20].

Figure 2.4: Schematic of the PVT with two different types of absorbers .

### 2.6.1 Economy and lifetime

Solar technology has in general a high investment cost, but a low operational and maintenance cost. The energy produced is in this way pre-paid, and the higher the electricity cost is more economically beneficial the system is.

PVTs has a much higher investment cost than ST and PV, but is a space-efficient way to implement both. Different sources states a lifetime of 20-30 years [21], [22] and negligible maintenance costs.

Communication with Gilbert Jensen in Carbon Neutral Energy gave some indication of prices for PVT:

Facilities over 30 kWp:

1. PVT: 2 200 - 2 600 EUR/kWp

Facilities less than 30 kWp:

1. PVT: 2 400 - 3 000 EUR/kWp

These prices are excluded VAT, and refers to both material and installation per installed kWp.

## 2.7 Seasonal thermal energy storage

A building's heating demand usually varies throughout the year. Solar technology has been used for a long time as a renewable energy source to cover parts of the heating load. The difficulty with solar energy is the availability of it, as it is a time-dependent energy source and does not always match the demand profile. The accessibility is usually at its best when the heating demand is at its lowest, especially in cold areas. A solution to the seasonal mismatch, is to store the solar heat during the summer until it is more needed in the winter. This is called seasonal storage. A promising way of thermal energy storage (TES) is underground, also called underground thermal energy storage (UTES)[3].

There are three typical types of UTES systems, depending on the geological, hydrogeological and other conditions on-site: aquifer TES (ATES), borehole TES (BTES) and cavern/pit TES (CTES)[23]. Other UTES systems are ducts in soil and water tank storage. This section will focus on BTES.

### 2.7.1 Borehole thermal energy storage

Borehole thermal energy storage (BTES) is an environmentally friendly technology that helps reduce the need for imported energy to a building. The BTES system allows storage of heat in the soil or rock in an array of borehole heat exchangers (BHE). The system is especially suitable for buildings with a relatively balanced heating and cooling load, but it is also applicable for buildings with mainly a heating load if the heat injection to the ground is replaced by another heat source. Other heat sources could be surrounding buildings with a cooling load or solar energy [3].

The BHs in BTES systems with rock or clay/soil are typically inserted with plastic pipes that have a "U"-bend at the bottom [3]. This is commonly used in Northern Europe and North America. Coaxial pipes and double U-pipes can also be used, which are more used in Central Europe [24]. A heat transfer fluid, usually an anti-freezing solution, is pumped around the BHE. The wells are then filled with a material

with a high thermal conductivity to ensure good thermal contact with the ground surrounding the pipes[3]. In European applications, groundwater is typically used as filling, whereas a grouting material (bentonite, concrete etc.) is more common in the US and Central Europe. A schematic sketch of a vertical BHE with a u-pipe can be seen in figure 2.5.

It is also possible to have a system where the heat transfer fluid has contact directly with the ground [25]. In a coaxial open BHE, a single pipe in the center of the well is used. This pipe carries the brine fluid to the bottom of the well. The surrounding space is then working as the outer coaxial conduct, and is the channel for the upwards flow. With an open solution like this, the fluid is in direct contact with the bedrock, leading to an efficient HX [26].

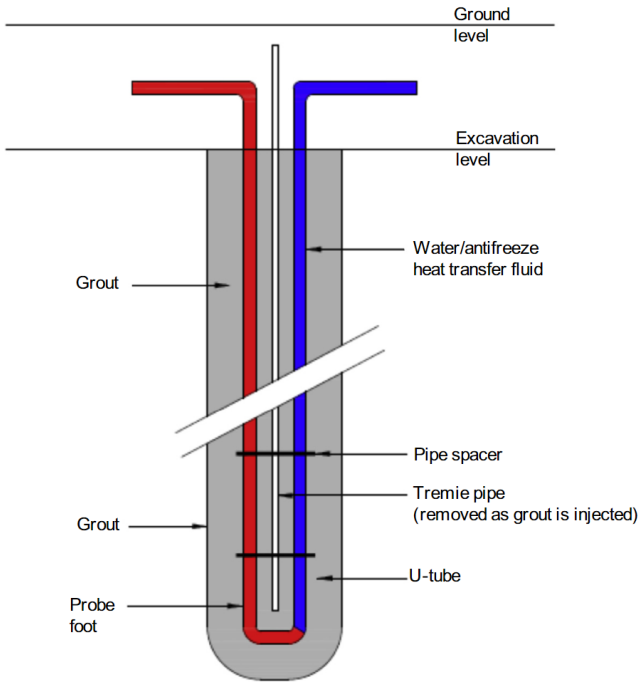


Figure 2.5: Schematic sketch of a BHE [3].

**Equations for borehole thermal energy storages**

The heat transfer between the BHE fluid and the surrounding ground is dependent on how the flow channels are arranged, the convective heat transfer in the channels, and the material involved in the thermal process' thermal properties [24]. The heat

flow in the BHE is dependent on the temperature difference and the thermal resistance between its carrier fluid and the wall of the BH. The influence of the thermal resistance is particularly crucial in, among others, low temperature applications with a high demand for high heat transfer rates at a small temperature difference. The definition of thermal resistance ($R_b$) between the heat carrier fluid and the BH wall can be seen in eq. 2.2.

It can be seen that the thermal resistance between the BHE and the BH wall depends on the temperature difference of the heat carrier and the wall, and the convective heat transfer between the BHE and the BH wall. A low flow rate usually induces a higher resistance, particularly if the BH is long [27]. The thermal resistance should be at a minimum to be able to extract as much energy as possible and to ensure a high quality BHE.

$$T_f - T_b = q \cdot R_b \tag{2.2}$$

$$T_f = \frac{1}{2}(T_{fin} + T_{fout}) \tag{2.3}$$

where:

$T_b$: Average ground temperature of the BH wall [$^\circ C$]

$T_f$: Mean temperature of the heat carrier fluid, according to eq.2.3, where $T_{fin}$ is the inlet fluid temperature and $T_{fout}$ is the outlet fluid temperature [$^\circ C$]

$q$: Heat injection/rejection rate [W/m]

The heat transfer rate is dependent on the heat transfer capacity and the temperature difference between the heat carrier fluid and the storage. During steady flux conditions it can be calculated with eq. 2.4 [27].The heat transfer capacity defines the heat transfer rate per unit temperature difference between the storage and heat carrier fluid. It is dependent on the thermal resistance, number of BHs and the depth of the BHs.

$$P = UA(T_f - T_{stk}) \tag{2.4}$$

Where:

$P$: Heat transfer rate to/from the storage [$W$]

$UA$: Heat transfer capacity [$W/K$]

$T_f$: Mean temperature of the heat carrier fluid (eq. 2.3)[$^\circ C$]

$T_{stk}$: Mean storage temperature [$^\circ C$]

The storage capacity ($C$) is another interesting quantity. It describes the maximum of thermal energy that the BTES can store, and it depends on the storage's maximum and minimum temperature throughout one year. It is also a subject to the integration of the storage in the system, operation and the type of system. Particularly, the maximum storage temperature is determined by the heat source's temperature level and the heat transfer capacity of the storage. The equation for calculating the storage capacity can be found in eq. 2.5 [27].

$$C = \rho c_f V (T_{stk,max} - T_{stk,min}) \tag{2.5}$$

Where:

$C$: Storage capacity $[J]$

$\rho c_f$: Mean ground volumetric thermal capacity $[J/m^3K]$

$V$: Storage volume $[m^3]$

$T_{stk,max}$: Maximum mean storage temperature $[^\circ C]$

$T_{stk,min}$: Minimum mean storage temperature $[^\circ C]$

The heat losses from the storage is mainly dependent on the mean annual storage temperature, mean ambient temperature, an equivalent heat loss factor and the surface area of the storage. With steady-state conditions, the heat losses from the BTES can be expressed as in eq. 2.6[27]. The time-dependent average heat loss factor depends on the design of the storage, such as insulation and geometry, and the properties of the ground. After a few years of operation, a steady-state thermal process will be established. Both free and forced convection in the ground increases the heat losses, but they can be reduced with insulating the top of the storage, vertical extension twice the storage diameter, and a low-temperature heat distribution. The latter will result in a lower storage temperature and thus a smaller heat losses.

$$Q_{loss} = UA(T_{stk,y} - T_{amb})t_y \tag{2.6}$$

Where:

$Q_{loss}$: Yearly heat loss from the storage $[kJ]$

$U$: Equivalent heat loss factor $[kW/m^2K]$

$A$: Surface area of the BTES $[m^2]$

$T_{stk,y}$: Mean annual storage temperature [$^{\circ}C$]

$T_{amb}$: Mean annual ambient temperature [$^{\circ}C$]

$t_y$: Duration of one year [$s$]

**Borehole configuration**

There are typically two ways of using the BHs: as a seasonal storage or as a heat source for a HP. With the first one, solar heat or heat from buildings are injected during the summer time and it usually requires several BHs. Several studies [28], [29], [30] have shown that BTES with one single BHE is not efficient. The reason for this is that the heat recharged will "leak" away rapidly, and the cost of extra circulation pumps and so will counterbalance the small thermal advantage [26]. When the BHs are used as a heat source for the HP, the ground is naturally recharged when there is no heating demand, and it typically only consists of one or two BHs.

Nordell and Helstrøm [31] states that the heat loss from a BHE is strongly dependent on its size and the temperature of the brine fluid. Most BTES designed for low temperatures, 10-40 °C, are typically supplied by glazed ST collectors and they are designed for solar fractions ranging between 50 and 90% [32]. To minimize losses, the BH field usually has a compact design with short wells. With an energy balance in the ground, the BHs are typically drilled in a square, hexagon or cylindrical array shape [26]. It is also possible to have smaller spacing between the wells, compared to when the BHs are only used for heating. This way the heat storage field of each BH will overlap (figure 2.6a) and the ratio between surface and volume will be minimized, and the heat loss is reduced. On the other hand, it is important to store enough solar thermal energy in the BTES with smaller spacing to avoid a decrease in temperature and performance.

If the BTES is only used for heating, it is important with enough surface area and the wells needs to be placed in individual rows with a spacing of minimum 15 m. An example of this can be seen in figure 2.6b. This could be complicated in densely populated areas. When there is thermal storage involved, the BHs can be placed closer, 6-8 m, in an array [3].

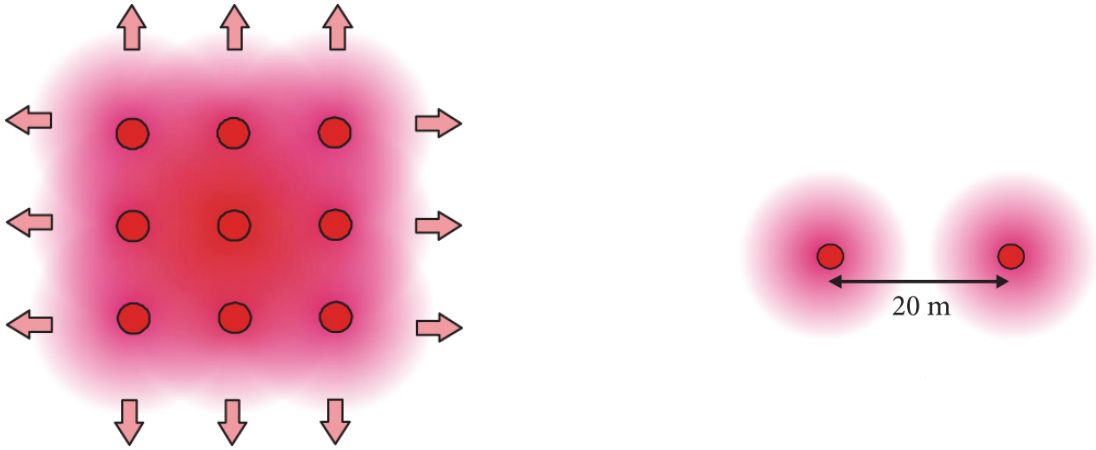


(a) A BTES field with a square array of BHEs [26].

(b) A BHE field spaced 20 m from each other [26].

Figure 2.6: Different configurations of BHE fields.

**Economy and lifetime**

An important aspect in the design of BTES and GSHP systems are the investment price of the BHEs. The price is highly dependent on factors such as the number of BHs, their depth, and geological properties. If the thickness of sediments covering the bedrock is large, it is necessary with steel castings to stabilize the ground, which is 3-5 times more expensive than drilling in bedrock [33]. The bedrock's thermal conductivity and temperature have an impact on the specific heat extraction, but does not affect the investment cost much due to the low drilling costs in bedrock.

The typical cost for drilling in bedrock is 150-250 NOK/m (ca. 12-22 EUR/m) excluded VAT, and one complete BHE that is 200 m deep typically costs 65 000-70 000 NOK (ca. 5 600-6 000 EUR). With 50 meter of sediments in addition, the price increases approximately 25 000 NOK. A BHE has a long lifetime of at least 40 years up till 100 years. Other advantages are that it is a reliable solution, it has a stable temperature which induces energy savings on the coldest days, and it is fitting for all facility sizes.

The cost of a brine-water HP is highly dependent on the size and performance. It usually ranges between 85 000-150 000 NOK (ca. 7 300-13 000 EUR) [34], and they have a lifetime of 20-30 years.

## 2.8 Performance and State-of-the-Art review

This section contains an overview of the performance of a GSHP and PVT-SAHP, as well as a state-of-the-Art review on the latter.

### 2.8.1 Ground-source heat pump

N. Sommerfeldt and H. madani [35] analyzed a GSHP located in Stockholm, Sweden in TRNSYS. The GSHP analyzed had 12 BHs with 20 m spacing and a depth of 275 m. The heat pump was a variable speed HP with a heating power of 52 kW. They achieved an SPF and SPF4 of 3.71 and 3.44 in year 1, and 3.56 and 3.27 in year 20, respectively. The research also showed that reducing the depth from 275 m to 110 m would require 13% more electricity.

### 2.8.2 Solar-assisted heat pumps

One of the first SAHPs was introduced by P. Sporn and E.R Ambrose in 1955 [36]. This was a direct-expansion SAHP (DX-SAHP) water-heater. With the DX-SAHP's efficient use of low temperature solar energy, the investigations of the system has the past decades advanced [37]. The PVT-SAHP dates back to 1981, when J. W. Andrews [38] evaluated its economical viability. For the system to be considered a promising alternative, it had to pass three tests: it had to be competitive with PV panels, ST collector, and side-by-side PV panels and ST collectors. The system was tested for both glazed and unglazed PVT collectors in Los Angeles, New York and Tampa. For collection of thermal energy, two technologies were considered: technology based on metal and glass, and technology based on thin-film plastics. The results showed that the glazed PVT was not a satisfactory alternative in any of the studied locations, and that the unglazed PVT was marginally an attractive option.

D. Sauter et al. [39] investigated how much regeneration is possible in districts with buildings supplied entirely by GSHP with thermal energy storage in Zurich. Both uncovered PVT and covered flat-plate collectors were used as sources for regeneration. The flat-plate collectors allowed for more regeneration than the PVT, and required 1.2 $m^2$ of collector area per MWh of heat demand to achieve full regeneration. PVT on the other hand required a collector area of 1.8 $m^2$ per MWh of heat demand.

N. Sommerfeldt and H. Madani [35] analyzed how PVT could reduce the size of the BH field. For a case with 12 BHs, the results showed that adding 236 $m^2$ of PVT improved the SPF by 2.5% and 6.8% with depths of 275 and 110 m, respectively.

Adding the same amount of PVT to 6 BHs with a depth of 275 m improved the average SPF by 4.8%. By reducing the BH spacing of a GSHP system with PVT, the SPF4 was mitigated. Further analysis on the effect of PVT showed that there is a diminishing return with increasing the PVT collector area, and that 79 $m^2$ of PVT can recover 85% of the reduction in SPF between a system without PVT and with 236 $m^2$ of PVT. In the same report, they analyzed how the size of the PVT collector affects the SPF4 for GSHP system with 6 BHs with a spacing of 5 m and depth of 200 m. The results showed an SPF4 of maximum 3 for all areas between 79 and 236 $m^2$ over 20 years.

In another study, N. Sommerfeldt and H. Madani [40] analyzed a GSHP with PVT in Sweden by using TRNSYS. The results showed that with PVT, the BH length could be reduced by 18% or the spacing by 50% compared to for a stand-alone GSHP, while still achieving the same seasonal performance. F. M. Rad et al. [41] examined the viability of a hybrid GSHP with ST for heating dominated buildings in TRNSYS. It was carried out a sensitivity analysis to determine the relationship between the BHE length and the ST collector area. The results showed that the length could be reduced by 4.7 m per $m^2$ of ST collector.

The first implementation of PVT-SAHP technology in Norway was Varden school in Bergen in 2017 [42]. The building was originally built in 1964 and was suffering with a high energy demand and a poor indoor environment. To improve this, the building was refurbished with 130 $m^2$ PVT collectors in synergy with a GSHP with BHs. The project was expected to have knock-on effects for the international energy efficiency.

Another ongoing project as of 2023 is Gartnersletta in Trondheim, Norway. It will be the worlds first Powerhouse housing, and will follow FutureBuilt's[43] definition of a plus house for energy production. By this, it has to produce a surplus of energy over the year [44]. In addition, the total greenhouse gas emissions needs to be lower than the lower limit of the Paris Proof agreement. The project consists of about 200 apartments from 40-120 $m^2$ and 200 $m^2$ of commercial area. The goals will be achieved by utilizing a large amount of PVT and BHs for seasonal storage.

Another ongoing project is Blå Port in Karskrona, Sweden. This is an apartment block with 10 floors and 57 apartments [45]. It has a goal of being a ZEB-O building, which means that renewable energy sources compensates for the greenhouse gas emissions during operation of the building. The project also has a goal of minimizing emissions during the construction phase, and to obtain valuable experience to reach the climate goals in upcoming projects. The building's roof will be covered with 40%

PVT and 60% PV. It will have a GSHP and BTES. The result is net zero energy use and a $CO_2$ footprint of 0 kg per year. During the construction phase, they have a climate action plan to reduce the climate impact. This is achieved by choosing climate-smart construction technology, and they have a goal of a climate footprint of 264 kg $CO_2/m^2$ of heated floor area during the construction phase.

## 2.9 Economic assessment

An economical analysis is often used to asses the financial viability of an action, such as providing a new product. Other use cases could be to compare two solutions to find the economically superior one. It is important to have a long term horizon, as investments and revenues does not appear at the same time. Especially GSHP and solar systems have a high initial cost, but provide savings for many years later on.

In this work, the biggest interest for the economical analysis is to compare different solutions. The total cost, investment and payback time is therefore calculated.

### 2.9.1 Discount rate

Discount rate can be distinguished between the nominal discount rate and the real discount rate[46]. The difference between them is that the real discount rate accounts for inflation. Other factors that may be corrected for with the real discount rate is relative energy price fluctuations and taxes[47].

### 2.9.2 Annuity

The annuity factor can be used to find the present value of payments. It is the sum of individual discount factors. The discount factor is calculated as $(1+r)^{-n}$, where n=1,2,3..k.

$$\varepsilon_{r,n} = \frac{r}{1-(1+r)^{-n}} \tag{2.7}$$

### 2.9.3 Investment

The investment cost is the cost that results in the acquisition of end items. It includes, but is not limited to, the costs of design, purchase, construction. The investment (I) can be calculated from eq. 2.8 as the sum of investments.

$$I = \sum_{i=1}^{n} I_i \tag{2.8}$$

### 2.9.4 Salvage value

Sometimes the horizon of the analysis is shorter than the lifetime of the asset, and it still has some value at the end of the analysis period [46]. This value must be taken into account, to treat different alternatives equally. There are many methods to use for depreciation, but in this report the focus will be on a linear one. The discounted salvage value can be calculated using eq.2.9, and it can be taken into account by subtracting it from the investment cost (eq. 2.10).

$$F_{R,0} = \frac{n-T}{n} \cdot (1+r)^{-T} \cdot F_0 \tag{2.9}$$

$$F_0' = F_0 - F_{R,0} \tag{2.10}$$

Where:

$F_{R,0}$: The salvage value referred to at the start of the analysis period [EUR]

$n$: Assumed lifetime of asset [$years$]

$T$: Time horizon for the analysis [$years$]

$r$: Discount rate [-]

$F_0$: Investment cost of the asset [EUR]

$F_0'$: Initial cost with salvage cost accounted for [EUR]

### 2.9.5 Total cost

The total cost is often used when it is desirable to do an economic assessment of different alternatives [46].The total cost is defined as the sum of the present values of fixed costs and variable costs. The fixed cost is typically investment costs, and the variable costs are typically operation dependent cost, namely operation costs and maintenance costs. The total cost can be calculated using eq.2.11.

$$TC = FC + VC \tag{2.11}$$

Where:

$TC$: Present value of total cost over the time horizon of the analysis [EUR]
$FC$: Present value of fixed cost over the time horizon of the analysis [EUR]
$VC$: Present value of variable cost over the time horizon of the analysis [EUR]

### 2.9.6 Pay-back time

The pay-back time is the period, $N_0$, it takes before the present value sum of all the income in the future is the same as the investment costs [47]. It can be calculated using eq. 2.12. As an investment criteria, the project is often accepted if the pay-back time is less than the lifetime of the asset.

$$N_0 = \frac{ln[(1 - \frac{I}{B} \cdot r)^{-1}]}{ln(1 + r)} \tag{2.12}$$

Where:

$N_0$: Pay-back time [years]

$B$: Savings [EUR/$year$]

$I$: Investment cost [EUR]

$r$: Discount rate [-]

# 3 Modeling in TRNSYS

This section contains information on the models used to simulate in TRNSYS. Three models in TRNSYS have been used: GSHP, GSHP with PVT, and PV. The models in TRNSYS and by this also the values for the parameters, besides the model with PV, have been provided by the co-supervisor. As the models used in TRNSYS in this work are the same as applied in the specialization project, this section thus contains parts from it [3].

## 3.1 Weather data

The weather data used to simulate the system is generated using Meteonorm 7.2 for Gardermoen, Oslo. The weather file consists of hourly values from a typical meteorological year (TMY). The weather station at Gardermoen does not measure solar radiation, and in cases like this Meteonorm interpolates data [3].

The temperature distribution over a year is illustrated in figure 3.1. The max, min and average temperatures are summarized in table 3.1. The total horizontal radiation can be seen in figure 3.2.

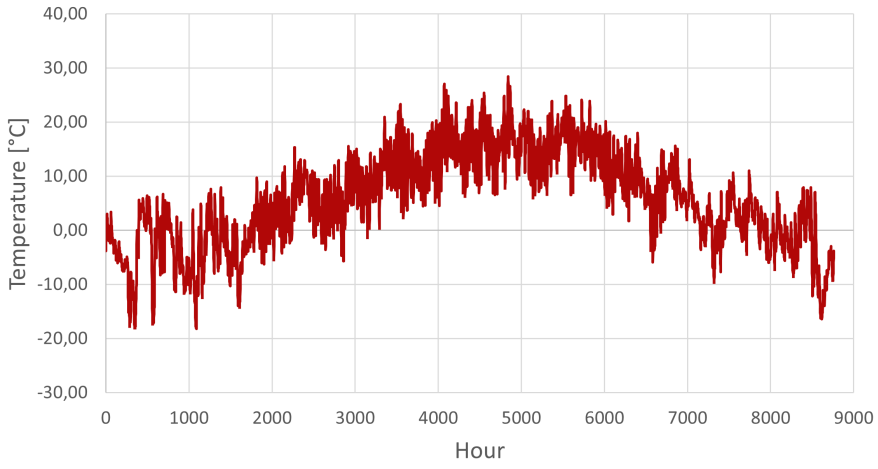


Figure 3.1: Ambient air temperature at Gardermoen, Oslo [3].

| | Temperature [°C] |
|---|---|
| Max | 28.40 |
| Min | -18.20 |
| Average | 5.68 |

Table 3.1: Max, min and average ambient air temperature.

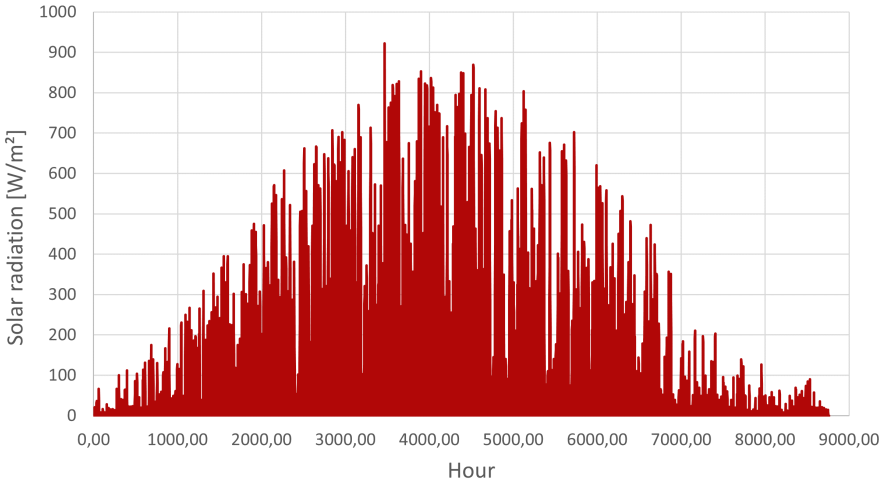


Figure 3.2: Total horizontal radiation at Gardermoen, Oslo [3].

## 3.2 Reference building

The building is an apartment block built between 1991-2000. The building has four floors of 60 m x 7 m with a total heated area of 1 680 $m^2$, and 24 $m^2$ of windows per floor. The building is located in Oslo, Norway.

The TRNSYS model of the building has been provided by the co-supervisor, who has used Tabula to collect data about the building's structure and HVAC system. To gain data about the building's internal gains, infiltration rate, ventilation and DHW demand, the Norwegian standard SN-NSPEK 3031:2020 [48] has been used. The U-values from Tabula [49] and the building's actual U-values can be found in table 3.2. According to Tabula, an apartment block from this decade is equipped with an exhaust ventilation without any recovery of heat, and it is heated with electricity in the form of heating panels. In this work, floor heating has been used instead. The set-point temperature of the heating system is 22 °C from 07:00-23:00, and the

remaining hours it is 20 °C. A fixed infiltration rate is used, and it is calculated to 0.21 $h^{-1}$ using eq. 3.1 from SN-NSPEK 3031:2020[48].

$$n_{inf} = \frac{n_{50} \cdot e}{1 + \frac{f}{e}\left(\frac{\dot{V}_1 - \dot{V}_2}{\dot{V} \cdot n_{50}}\right)^2} \tag{3.1}$$

| Building component TRNSYS model | Tabula value |
|---|---|
| U-value roof 0.27 $W/(m^2K)$ | 0.20 $W/(m^2K)$ |
| U-value external wall 0.29 $W/(m^2K)$ | 0.29 $W/(m^2K)$ |
| U-value external floor 0.27 $W/(m^2K)$ | 0.25 $W/(m^2K)$ |
| U-value window 2.43 $W/(m^2K)$ | 2.40 $W/(m^2K)$ |

Table 3.2: U-values from Tabula and the building.

### 3.2.1 Internal gains

For heat gain and power use related to people, lighting and technical equipment, schedules from SN-NSPEK 3031:2020 [48] have been used. They have been scaled to implement them in TRNSYS, but the unscaled ones can be seen in figure 3.3.

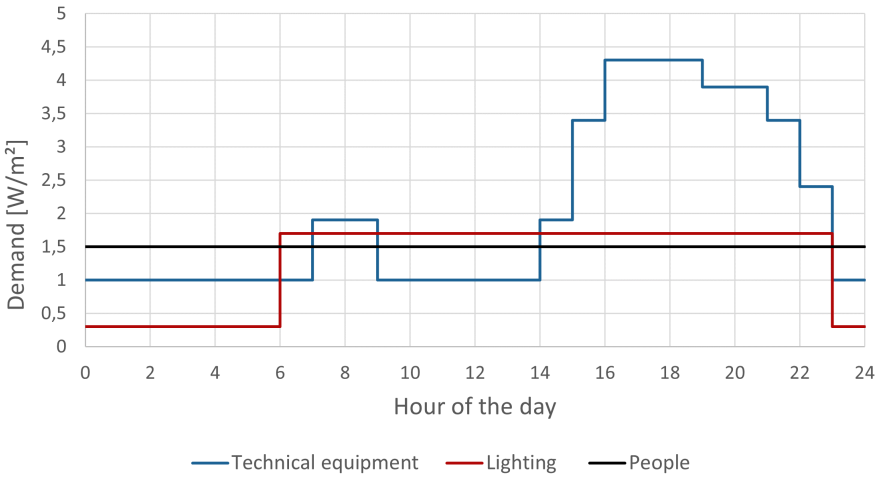


Figure 3.3: Schedule for the heat gain and power use from people, lighting and technical equipment [3].

### 3.2.2 Domestic hot water

The usage of DHW has been implemented according to the schedule in the Norwegian Standard [48], which can be seen in figure 3.4 [3].

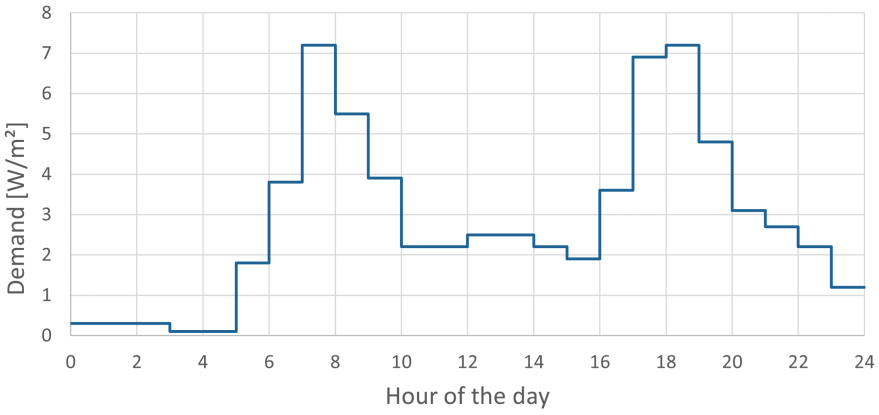


Figure 3.4: Schedule for use of domestic hot water [3].

## 3.3 Heat load

This section contains the heating load of the building, which was found in the specialization project [3]. The simulated heating demand was also during the project compared to data from Tabula. The duration curve for the resulting heating demand for space heating in TRNSYS can be seen in figure 3.5. From the curve, it can be observed that the building has a net power demand around 80 kW at DOT. In table 3.3, it can be seen that the heating demand in TRNSYS deviates from the Tabula data with -5.98%.

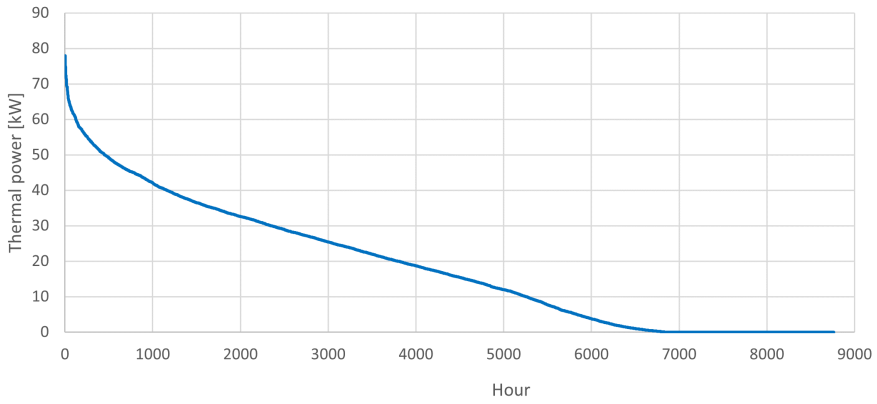


Figure 3.5: Duration curve for the building's simulated SH demand in TRNSYS.

| | Specific value TRNSYS $[kWh/m^2]$ | Specific value Tabula $[kWh/m^2]$ | Error TRNSYS [%] |
|---|---|---|---|
| SH | 106.7 | 114.8 | -7.03 |
| DHW | 25.0 | 25.3 | -1.19 |
| Total | 131.7 | 140.1 | -5.98 |

Table 3.3: Specific heating demands for the building from simulations in TRNSYS in comparison to Tabula.

From figure 3.6 it can be seen that the peak for heating happens in January, February and December, but there is a need for space-heating throughout most of the year. The exception is from June to August, where the heating demand is nearly exclusively characterized by heating of DHW. This is because the need for space-heating is closely related to the temperature difference between indoor and outdoor, which is the largest during the winter months [3].

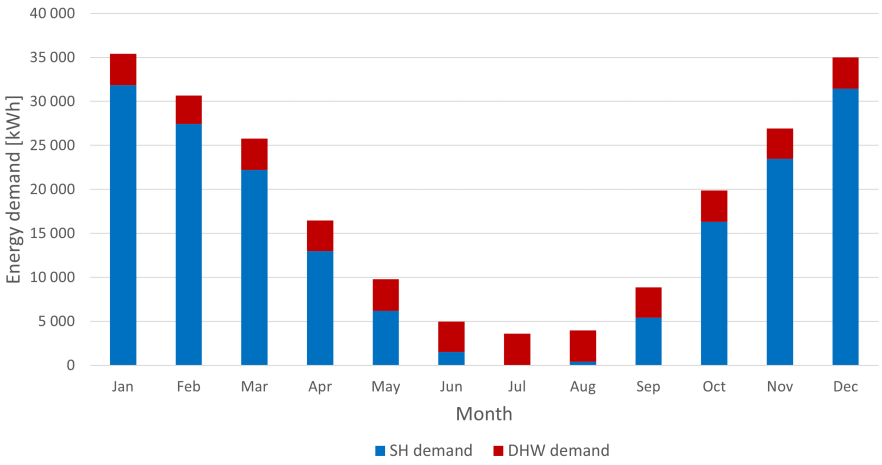


Figure 3.6: The building's heating demand in TRNSYS.

## 3.4 Main components

This section contains information about the main components and the data used for their parameters in TRNSYS.

### 3.4.1 Heat pump

The heat pump component that has been used is a single stage water-water HP (Type 927), from TESS GHP library. This HP model produces results based on user-supplied data file containing catalog data from the manufacturer[3] for heating and cooling performance. This data consists of the capacity and power draw as a function of the source and load temperatures that are normalized to the rated conditions [50]. The component is able to interpolate within the input values of the data file. As it is a single stage HP, it is on/off controlled, and operates at its full capacity when it is on. The heat pump DAIKIN-WHA 120 was chosen by the co-supervisor for the models and simulations. Only a heating performance data file is provided, as the HP is not used for cooling.

If the heat pump receives a signal to be turned on in heating mode, it calls the TRNSYS data subroutine with the load and source fluid entering it [51]. The routine then accesses the user-supplied data file, and the HPs heating capacity and power consumption is returned. The COP is calculated with eq. 3.2, and eq. 3.3 gives the energy absorbed in heating mode from the source fluid.

$$COP = \frac{Cap_{heat}}{\dot{P}_{Heating}} \tag{3.2}$$

$$\dot{Q}_{absorbed} = Cap_{heat} - dotP_{Heating} \tag{3.3}$$

Where:

$COP$: Coefficient of performance of the HP

$Cap_{heat}$: The HPs heating capacity at present state $[kJ/hr]$

$\dot{P}_{Heating}$: Power consumption by the HP $[kJ/hr]$

$\dot{Q}_{absorbed}$: Absorbed energy in heating mode $[kJ/hr]$

The HP is dimensioned to cover 70% of the peak heat demand. HPs are usually not designed to cover the entire peak heat load, as the peak only occurs a few times during a year. Due to the high specific investment cost of HPs, a HP designed to cover the whole peak heat demand would be unnecessary expensive with regards to investment. To cover the remaining heat load, the storage tanks for DHW and SH are equipped with auxiliary heating. The values for the HP's parameters can be found in table 3.4 [3].

| Parameter | Value | Unit |
|---|---|---|
| Rated heating capacity | 69.4 | $kW$ |
| Rated power capacity | 14.7 | $kW$ |
| Rated source flow rate | 5 110 | $kg/hr$ |
| Rated load flow rate | 5 110 | $kg/hr$ |
| Source fluid specific heat | 3.72 | $kJ/(kg \cdot K)$ |

Table 3.4: Parameter values used for the HP in TRNSYS [3].

### 3.4.2 Photovoltaic panel

The component used for the PV panel is a covered PV that bases its performance calculations on a overall array efficiency (Type 562d) from TESS electrical library [50]. The efficiency could either be constant or variable as a function of the cell temperature and incident radiation from an external file. It can also be provided for reference conditions with coefficients describing what the effects of any changes in cell temperature or incident radiation are. It is an appropriate choice when the PV is not connected to a load. The angle of slope for the PV is 44 °. Parameters

used for the PV are retrieved from DualSun's FLASH 425 Shingle Black [52] and a summary is shown in table 3.5. The rest of the parameters have been kept as their default values.

| Parameter | Value | Unit |
|---|---|---|
| Area | 100, 200, 300 | $m^2$ |
| Reference PV efficiency | 20.4 | % |
| Reference temperature | 25 | $°C$ |
| Reference radiation | 1000 | $W/m^2$ |
| Cover thickness | 32 | $mm$ |
| Slope | 44 | ° |

Table 3.5: Input values used for the PV in TRNSYS.

### 3.4.3 Photovoltaic-thermal collector

The PVT collector used for the simulations is a PVT collector that interacts with simple zone models (Type 560) from TESS electrical library. The component models an unglazed solar collector that consists of embedded PV cells and an absorber plate beneath the PV cells. The PV cells generates power, and a fluid stream in tubes bonded to the absorber plate collects waste heat. The angle of slope for the PVT is 44 °[3]. Collection of the waste heat has two useful reasons: 1) the PV cells are cooled down which allowas for a better efficiency and 2) the low-temperature heat can be utilized as a heat source [53]. The parameters and their values can be seen in table 3.6. The collector's useful energy gain is calculated with eq. 3.4 and the PV efficiency is given by eq. 3.5.

$$Q_u = \dot{m} C_p (T_{fluid,out} - T_{fluid,in}) \tag{3.4}$$

Where:

$Q_u$: Energy transfer rate to the flow stream in the collector $[kJ/kr]$

$\dot{m}$: Flow rate in the collector $[kg/hr]$

$T_{fluid,out}$: Temperature of fluid flow leaving the collector $[°C]$

$T_{fluid,in}$: Temperature of the fluid flow entering the collector $[°C]$

$$\eta_{PV} = \eta_{nominal} \cdot (1 + Eff_T(T_{PV} - T_{ref})) \cdot (1 + Eff_G(G_T - G_{ref})) \tag{3.5}$$

Where:

$\eta_{PV}$: Efficiency of the PV cell [-]

$\eta_{nominal}$: PV efficiency at reference conditions [-]

$T_{PV}$: Temperature of the PV cell [$°C$]

$T_{ref}$: Temperature at reference conditions [°C]

$G_T$: Incident total solar radiation on the solar collector [$kJ/hrcdotm^2$]

$G_{ref}$: Incident total solar radiation at reference conditions [$kJ/hrcdotm^2$]

$Eff_T$: Efficiency modifier for temperature [$1/K$]

$Eff_G$: Efficiency modifier for radiation [$hr \cdot m^2/kJ$]

| Parameter | Value | Unit |
|---|---|---|
| Collector length | 1.658 | $m$ |
| Collector width | $0.992 \cdot N_{col}$ | $m$ |
| Absorber plate thickness | 0.003 | $m$ |
| Thermal conductivity of the absorber | 720 | $W/(m \cdot K)$ |
| Number of tubes | $6 \cdot N_{col}$ | - |
| Tube diameter | 0.012 | $m$ |
| Bond width | 0.012 | $m$ |
| Bond thickness | 0.003 | $m$ |
| Bond thermal conductivity | 45 | $W/(m \cdot K)$ |
| Resistance of substrate material | 0.015 | $(m^2 \cdot K)/W$ |
| Resistance of back material | 0.00001 | $(m^2 \cdot K)/W$ |
| Fluid specific heat | 3.72 | $kJ/(kg \cdot K)$ |
| PV efficiency at reference condition | 0.1702 | - |
| Efficiency modifier - temperature | -0.0041 | $K^{-1}$ |
| Slope | 44 | $^\circ$ |

Table 3.6: Input values used for the PVT in TRNSYS. $N_{col}$ is here the number of collectors [3].

### 3.4.4 Boreholes

A vertical U-tube ground HX (Type 557a) from TESS GHP library is used to model the BHEs in TRNSYS. This model is the most common BHE used in GSHP systems, and it models a HX that interacts thermally with the ground. A fluid is circulated in the BHEs and it injects/rejects heat, depending on the temperature difference between the fluid and ground [3].

The model assumes that the BHs are placed uniformly within a cylindrical storage volume of the ground. It also assumes that within the pipes there is convective heat transfer, and that there is conductive heat transfer to the storage volume. To calculated the temperature in the ground, the problem is split into several parts; a global temperature and local solution that are solved using an explicit finite difference method, and a steady-flux solution that is obtained analytically. By using superposition methods, the ground temperature is then calculated [3].

| Parameter | Value | Unit |
|---|---|---|
| Number of boreholes | 8, 12, 16 | - |
| Borehole spacing | 20 | $m$ |
| Borehole depth | 200 | $m$ |
| Header depth | 2 | $m$ |
| Borehole radius | 0.075 | $m$ |
| Storage thermal conductivity | 2.62 | $W/(m \cdot K)$ |
| Outer radius of U-tube pipe | 0.02 | $m$ |
| Inner radius of U-tube pipe | 0.0185 | $m$ |
| Center-to-center half distance | 0.04 | $m$ |
| Fill thermal conductivity | 0.85 | $W/(m \cdot K)$ |
| Pipe thermal conductivity | 0.38 | $W/(m \cdot K)$ |
| Reference temperature | 10 | $^\circ$ C |
| Fluid specific heat | 3.72 | $kJ/(kg \cdot K)$ |
| Number of simulation years | 20 | years |
| Maximum storage temperature | 25 | $^\circ$ C |
| Initial surface temperature of storage volume | 5.7 | $^\circ$ C |
| Thermal conductivity of layer | 2.62 | $W/(m \cdot K)$ |

Table 3.7: Values used for parameters for the BHE field in TRNSYS [3] .

### 3.4.5 Pumps

To model the pumps, both on the source and load side, a pump component with variable flow rate has been used (Type 3b). The only parameters that have been changed for the pumps are the maximum flow rate and the maximum power [3].

The maximum flow rate and power for the pump in the BHE circuit are decided by the rated source flow and heating power for the HP. The maximum power for the pump is estimated to be approximately 4% of the rated heating power for the HP [3], which leads to an amount of 590.96 W .

The flow rate and power consumption for the pump in the PVT circuit is depending

on the collector area. The flow rate is set to $(50 \cdot A_{col})\ kg/hr$, and the power consumption is dependent on the size of the PVT collector and has a value of $50 \cdot A_{col} \cdot 0.0174$ $W$. The pumps on the load side have constant values of 5 110 $kg/hr$ and 88 $W$ for the flow rate and power, respectively.

# 4 Simulations in TRNSYS

## 4.1 Key Performance Indicators

To evaluate a system's performance, several key performance indicators (KPIs) exist, like seasonal performance factor (SPF), coefficient of performance (COP), and energy efficiency ratio (EER). COP is used for evaluating a heat pump when it is operating in heating mode, and EER when it is operated in cooling mode. The SPF is used to express the performance over time, like for an entire year or a season. This section was written during the specialization project [3].

### 4.1.1 Regeneration fraction

The regeneration factor is the ratio between the heat that is injected to the BTES by the use of solar energy or a cooling demand, and the heat that is extracted from the BTES with a HP. The equation to calculate it can be found in eq. 4.1. The heat injected ($\dot{Q}_{inj}$) is in this case the heat available on the source-side, after the HX between the PVT/ST and BTES, when there is no heat demand. The extracted heat ($\dot{Q}_{ext}$) is the heat used on the source-side of the HP.

$$Reg_{frac} = \frac{\int_0^t \dot{Q}_{inj}}{\int_0^t \dot{Q}_{ext}} \tag{4.1}$$

### 4.1.2 Average borehole temperature

The average temperature in the BHS ($T_m$) is the mean value of the inlet and outlet temperature of the BHs (eq. 4.2).

$$T_m = \frac{T_{in} + T_{out}}{2} \tag{4.2}$$

### 4.1.3 Seasonal performance factor

The seasonal performance factor (SPF) is a seasonal metric that uses measurements from typically a whole year or a season to evaluate the system's performance. It is not very useful for rating the equipment or the integration of the system, as it is sensitive to the ambient air temperature, but it is a good indicator for comparing different system solutions [54]. There are four different types of SPF, depending on the supplementary electrical demands, such as circulation pumps and supplementary heaters, that is included. In this report, SPF and SPF4 are considered. SPF only

takes account for the heat pump equipment, while SPF4 considers all circulation pumps and additional heaters [54].The equations for SPF and SPF4 can be seen in equation 4.3 and 4.4, respectively. All the inputs to the equations are integrated over the simulation period in question.

$$SPF = \frac{\int_0^t \dot{Q}_{HP}}{\int_0^t \dot{W}_{HP}} \tag{4.3}$$

$$SPF4 = \frac{\int_0^t (\dot{Q}_{SH} + \dot{Q}_{DHW})}{\int_0^t (\dot{W}_{HP} + \dot{E}_{SH} + \dot{E}_{DHW} + \dot{E}_{pumps})} \tag{4.4}$$

Where: $Q_{HP}$ is the heat released at the condenser of the HP, and $\dot{W}_{HP}$ is the power consumed by the compressor in the HP. $\dot{Q}_{DHW}$ and $\dot{Q}_{SH}$ are the heat demands for DHW and SH. $\dot{E}_{SH}$, $\dot{E}_{DHW}$ and $\dot{E}_{pumps}$ are the electrical power inputs for SH, DHW and the circulation pumps.

## 4.2 Model 1: Ground-source heat pump

Model 1 is a system with a GSHP, that the models with PV and PVT will be compared to. The layout of the model can be seen in figure 4.1. The red lines indicates warm flows and the blue lines cold flows. The modeling of the system as a whole in TRNSYS can be found in appendix A.1.

To get a better understanding of the functionality of the different parts of the model and their modeling in TRNSYS, the model will be split into a source side and a load side in this section.

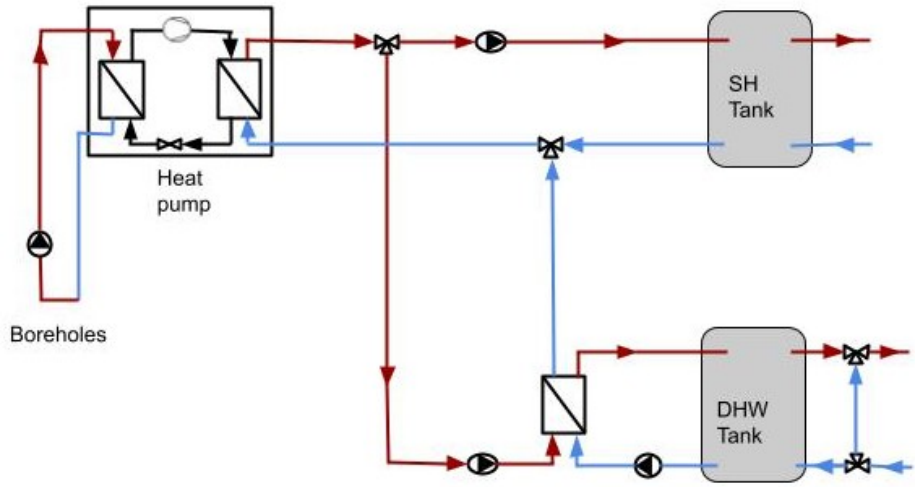


Figure 4.1: System sketch of model 1 [3].

### 4.2.1 Source side

The source side consists of a BHE field, a circulation pump and control, and can be seen in figure 4.2. The flow rate in the circuit is fixed, and is controlled by the required flow rate of the HP. A summary of the values used for the components on the source side is given in table 4.1, and more information on the setup of the components is given in section 3.4.

The circulation pump is a variable speed pump, and the flow rate is the same as the flow rate demand of the HP and it is controlled by the HP. If the HP is operating, the pump will be turned on. The most interesting outputs from the source side are the inlet- and outlet temperature of the BHs and average heat transfer rate.

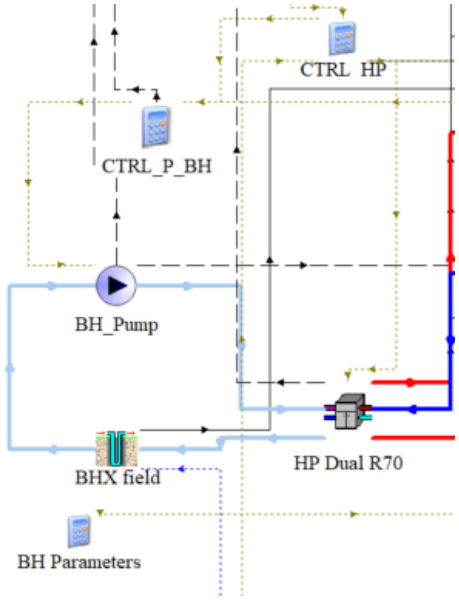


Figure 4.2: The source side of the TRNSYS model for the base case.

| Component | Parameter | Value | Unit |
|---|---|---|---|
| BHE field | | | |
| | Number of BHs | 8, 12, 16 | - |
| | Depth | 200 | $m$ |
| | Spacing | 20 | $m$ |
| Circulation pump | | | |
| | Maximum flow rate | 5 110 | $kg/hr$ |
| | Maximum power | 590 | $W$ |

Table 4.1: Main parameter values used for the source side of the base case.

### 4.2.2 Load side

The load side of the system consists of pumps, storage tanks and a HX, and can be seen in figure 4.3. The main parameters that have been changed and their values are summarized in table 4.2, and more information can be found in section 3.4.

The SH and DHW requires different temperatures, and the HP has a shuttle valve design. The control signal will prioritize heating of DHW and the SH-circuit has a storage tank to accumulate hot water. The use of a storage tank will additionally reduce the number of times the HP has to be switched on and off. Between the

storage tank and the HP, there is a HX. The auxiliary heaters in the tanks will be used when the HP cannot provide with a sufficient amount of heat, and to heat the DHW from 55 °C to 60 °C.

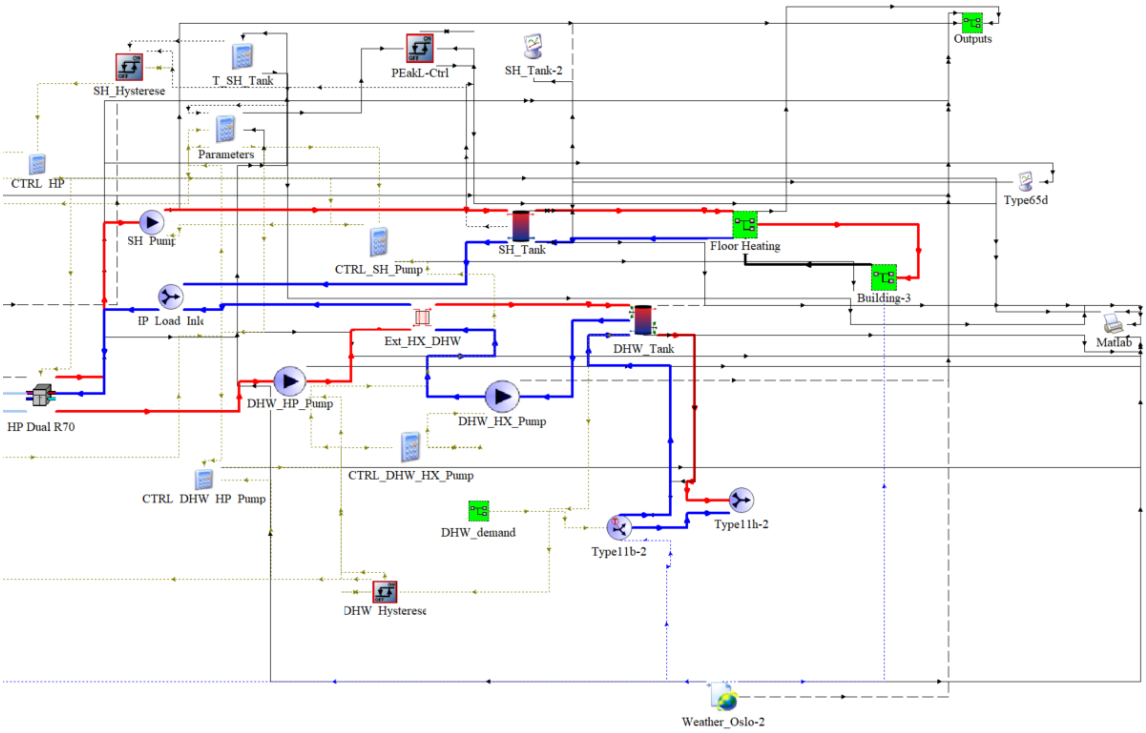


Figure 4.3: The load side of the TRNSYS model for the base case.

| Component | Parameter | Value | Unit |
|---|---|---|---|
| SH storage tank | | | |
| | Tank loss coefficient | 0.83 | $W/(m^2 \cdot K)$ |
| | Auxiliary heater | 40 | $kW$ |
| | Volume | 5 | $m^3$ |
| DHW storage tank | | | |
| | Tank loss coefficient | 0.83 | $W/(m^2 \cdot K)$ |
| | Auxiliary heater | 10 | $kW$ |
| | Volume | 1.75 | $m^3$ |
| Circulation pumps, SH and before HX DHW | | | |
| | Maximum flow rate | 5 110 | $kg/hr$ |
| | Maximum power | 88 | $W$ |
| Circulation pump, after HX DHW | | | |
| | Maximum flow rate | 3 000 | $kg/hr$ |
| | Maximum power | 55 | W |
| DHW HX | | | |
| | UA | 12 000 | $W/K$ |

Table 4.2: Main parameter values used for the load side of the base case.

**Floor heating**

The model provided by the co-supervisor is equipped with floor heating that is inserted as an active layer in the ground of the building. The floor heating of each zone is PID-controlled, and the controlled variable is the air temperature of each zone in the building, that is measured by a thermostat. The control of the floor heating in TRNSYS can be seen in figure 4.4.

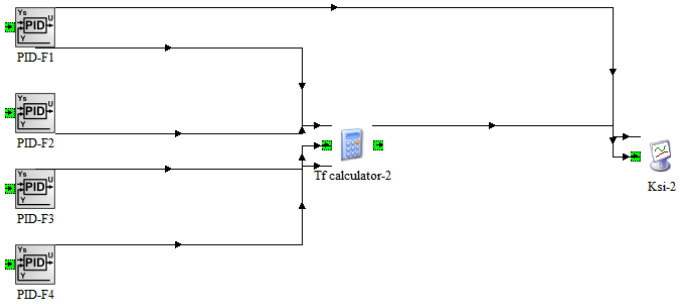


Figure 4.4: The control of floor heating in TRNSYS.

For the supply-temperature of the SH to better match the demand temperature at

other conditions than the design temperature, a heating curve has been implemented. The equation for the curve can be seen in eq. 4.5, and and figure 4.5 shows an illustration of it.

$$y = -0.375 \cdot x + 35 \tag{4.5}$$

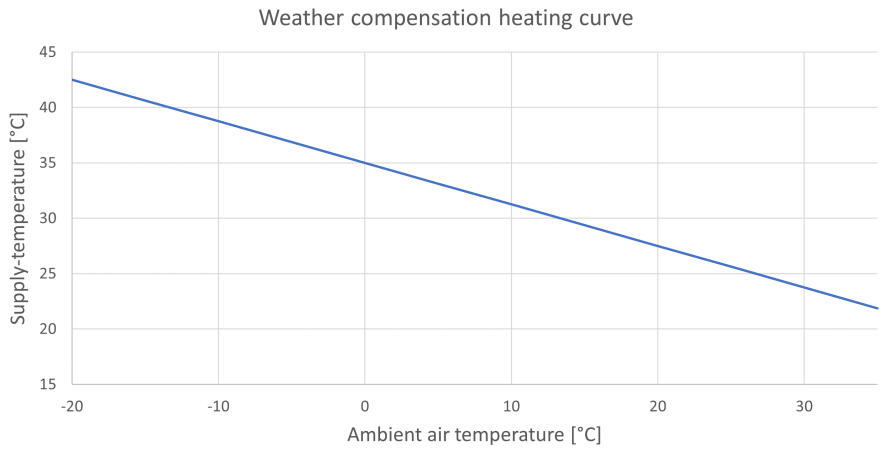


Figure 4.5: The heating curve applied to the setpoint temperature of SH.

### 4.2.3 Control

**Domestic hot water**

The heating of DHW is controlled by the temperature at node 4 in the DHW storage tank with temperature hysteresis (an aquastat). If the temperature is 3 K below the setpoint temperature of 55 °C, the pump before and after the HX will receive a signal to turn on. The pumps will receive a signal to be turned off when the temperature is 4K above the setpoint temperature. This is used to avoid wear and tear from toggling on and off on both the HP and the pumps.

**Space-heating**

The pump in the SH circuit is controlled by the DHW pump and temperature hysteresis. The setpoint temperature is controlled by a heating curve, described in section 4.2.2. The aquastat will send an on-signal to the pump when the temperature of node 9 the tank is 2 K lower than the setpoint, and off when it is 2 K higher. In addition, the heating of SH water with the HP will not occur if preparation of DHW is taking place.

**Auxiliary heating**
There are two auxiliary heaters: one in the SH tank and one in the DHW tank. The heater in the DHW tank will turn on when the temperature at node 1 in the tank is 4 K below the setpoint of the heater, which is 60 °C. It turns off when the temperature of the water reaches the setpoint. The heater is located at node 2.

The heater in the SH tank is located at node 2. This heater is controlled by temperature hysteresis, and will be turned on when the temperature at node 1 is 1 K below the heating curve, and off when it is 1 K above the heat curve.

**Heat pump and borehole field**
The HP and the pump in the BHE circuit will be turned on if the temperature falls below the setpoint temperature and off when it is above, according to the hysteresis of the SH and DHW.

### 4.2.4 Results

The system described in section 4.2 has been simulated with 8, 12 and 16 BHs. Simulations over 1 year and 20 years with a time-step of 2 minutes have been carried out to investigate how the different variants behave both short- and long-term. Model 1 is the base case.

The energy demand and extracted heat for the variants of the base case over the first year can be seen in figures 4.6 and 4.7. With more BHs, the amount of heat extracted is increased, which is reflected in the reduced amount of auxiliary heating for SH. The auxiliary heating for DHW is the same all year. This is because of the priority of DHW and the small amount of energy consumed is from heating the water from 55°C to 60 °C.

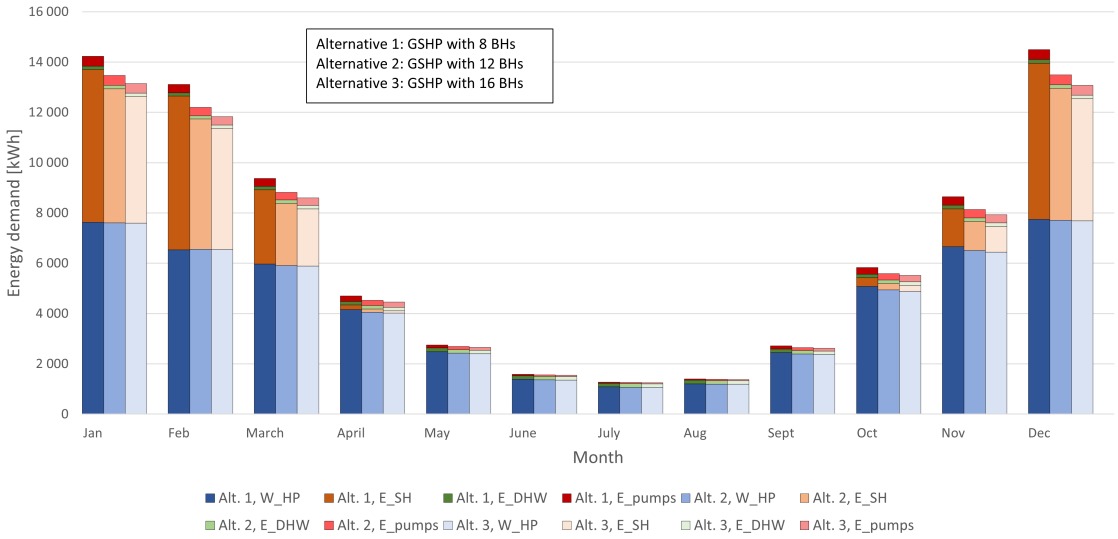


Figure 4.6: Energy use for model 1.

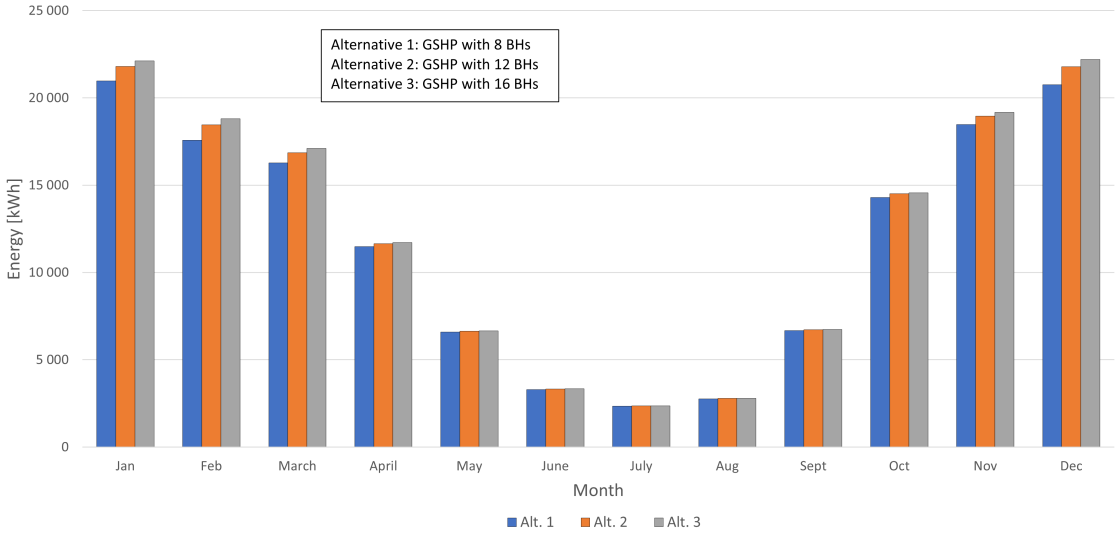


Figure 4.7: Extracted energy for model 1.

The first year, the SPF and SPF4 illustrated in figure 4.8 ranges from 3.16-3.98 and 2.28-3.54, respectively. The highest SPF4 is achieved during the fall and spring, when there is a moderate DHW and SH demand. It is at its lowest when there is

only a DHW need during the summer and when the heating demand is at its highest. The difference in performance between the three alternatives is the most noticeable September to April, due to the difference in heat extracted from the BHE field. In the summertime, the heat demand is low and almost exclusively for DHW, which results in a low SPF4. In the winter, the SPF4 is lower due to the auxiliary heating for especially SH. SPF has the same tendencies, except for the reduction during the coldest months. This is likely because it does not include auxiliary heating. Its reduction in the summer is caused by the small heating load and because it is only able to operate at its full capacity.

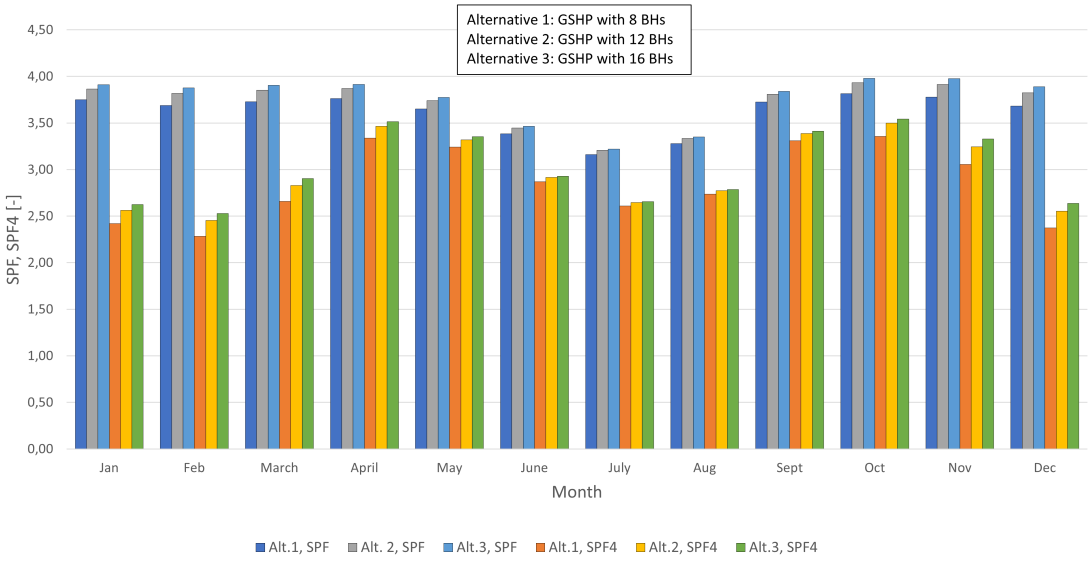


Figure 4.8: SPF and SPF4 for model 1.

**Long term results**

In cold climates, it is acceptable that the temperature of the collector fluid is a few degrees below freezing, as it still provides a better performance than an air-sourced HP [3]. From table 4.3 it can be seen that after 20 years the minimum average fluid temperature ($T_m$) with 8 BHs is -2.27 °C.

The SPF and SPF4 in year one is in the range of 3.70-3.87 and 2.68-2.91 for all the GSHP systems. Sommerfeldt and Madani [35] found the SPF and SPF4 to be 3.71 and 3.44 in year 1 and 3.56 and 3.27 in year 20, with a similar building and 12 BHs with a depth of 275 m. This is a higher SPF4 than what is achieved in this case, but

a possible explanation could be deeper BHs and other differences in the simulation models.

The SPF and SPF4 is reduced by roughly 3-5% and 5-9%, respectively, from year one to year 20 for the different number of BHs. The system with 8 BHs has the largest descend, and this is likely due to a smaller surface area of the BHE field and less BHs to extract heat from, which leads to a faster decrease in temperature. Increasing the number of BHs by 50% from 8 to 12 lifts the SPF and SPF4 by 4.58% and 7.79 %, respectively. By doubling the number of BHS from 8 BHs to 16 BHs, the SPF and SPF4 rises by 7.16% and 12.30%.

| Number of BHs | Year | SPF [-] | SPF4 [-] | Minimum $T_m$ [° C] |
|---|---|---|---|---|
| 8 | 1 | 3.70 | 2.68 | 0.07 |
| | 20 | 3.49 | 2.44 | -2.27 |
| | Avg. | 3.57 | 2.53 | -0.04 |
| 12 | 1 | 3.82 | 2.84 | 1.89 |
| | 20 | 3.65 | 2.63 | -0.04 |
| | Avg. | 3.72 | 2.71 | 1.66 |
| 16 | 1 | 3.87 | 2.91 | 2.73 |
| | 20 | 3.74 | 2.74 | 1.04 |
| | Avg. | 3.79 | 2.81 | 2.45 |

Table 4.3: Summary of the KPIs for the GSHP over 20 years.

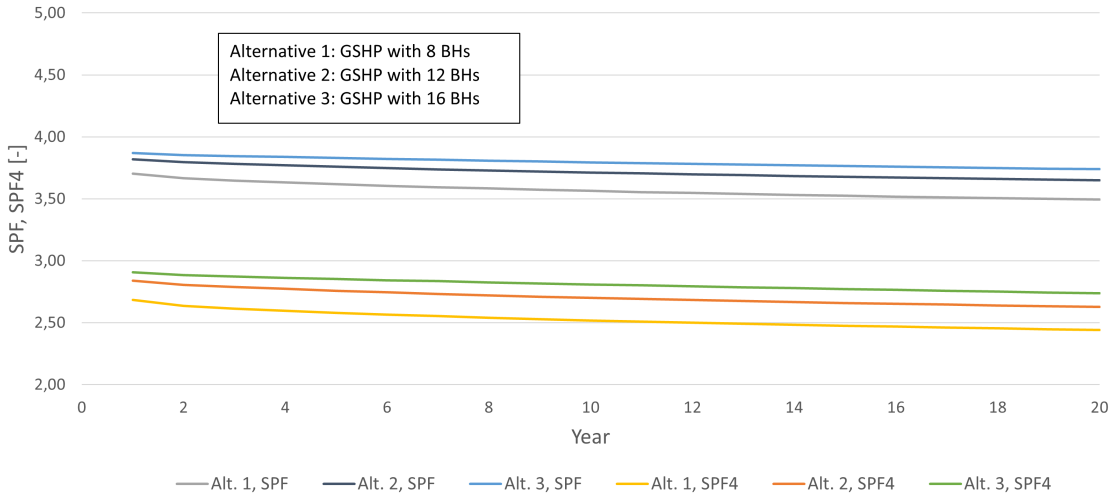


Figure 4.9: KPIs for the GSHP system the first 20 years.

The lower KPIs in year 20 can be explained by a gradually decrease in the average fluid temperature in the BHs, and it can be seen in figure 4.10 for 12 BHs. It is worth noticing that it has not reached a steady-state after 20 years. With a lower average fluid temperature in the BHs, less heat will be extracted and a larger part of the heat demand will be covered by the peak-load heating system. It can be seen in figure 4.9 that the decrease in the KPI's have not reached a steady-state either after 20 years.

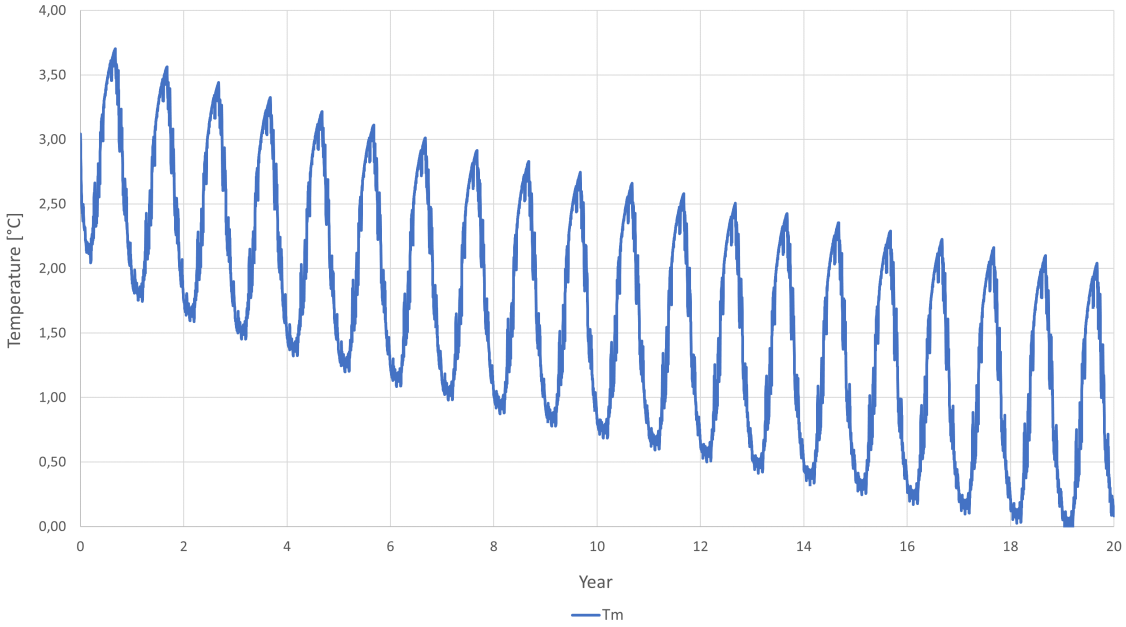


Figure 4.10: Average brine fluid temperature for the GSHP system with 12 BHs the first 20 years.

## 4.3 Model 2: Ground-source heat pump and photovoltaic-thermal collector

Model 2 is based on the base case, and the load side of the HP remains the same as for model 1, described in section 4.2.2.

In this model, the building and floor-heating have been replaced by a load-file to improve the simulation time. The system sketch for model 2 can be seen in figure 4.11, where blue lines represents cold flows and red lines represents warm flows.

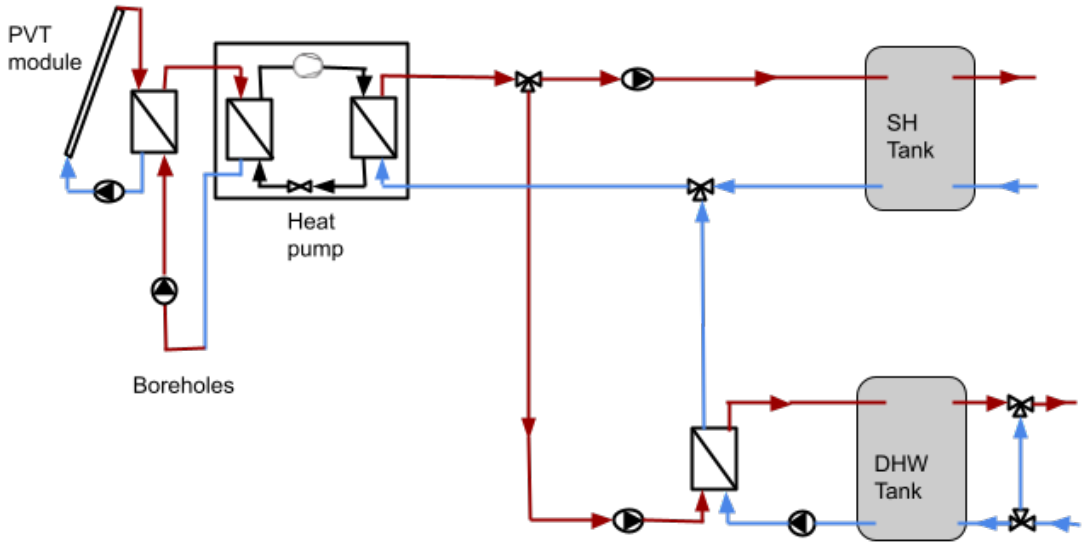


Figure 4.11: System sketch of the system with a GSHP and PVT [3].

### 4.3.1 PVT circuit

The PVT circuit consists of a circulation pump, a HX, the PVT and control. Figure 4.12 shows the circuit in the TRNSYS model, and the PVT component is described in section 3.4.3. The main parameters are summarized in table 4.4

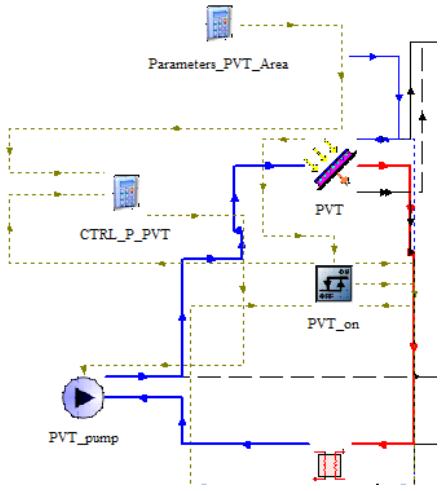


Figure 4.12: The PVT circuit in the TRNSYS model of case 1.

| Component | Parameter | Value | Unit |
|---|---|---|---|
| PVT | | | |
| | Collector length | 1.658 | $m$ |
| | Collector width | $0.992 \cdot N_{col}$ | m |
| | Number of tubes | $6 \cdot N_{col}$ | - |
| | Slope | 44 | $^\circ$ |
| Circulation pump | | | |
| | Maximum flow rate | $50 \cdot A_{col}$ | $kg/hr$ |
| | Maximum power | $50 \cdot A_{col} \cdot 0.0174$ | $W$ |
| HX | | | |
| | UA | $80 \cdot A_{col}^2$ | $W/K$ |

Table 4.4: Main parameters and their values used for the PVT circuit.

The pump in the PVT circuit is controlled by the temperature of the BHE fluid and temperature at the PVT outlet. The pump is operating when the outlet temperature of the fluid in the PVT circuit is 6 K higher than the outlet temperature from the BHs, and it is turned off again when it is 1 K lower. If the temperature requirement is met, the PVT circuit will provide heat to the BH circuit, and if there is no heat demand from the HP, the solar heat will be used for regeneration of the BHE field.

### 4.3.2 Regeneration of the BTES

The BTES circuit with a BHE field, a HX, a circulation pump and the HP can be seen in figure 4.13. The most important parameters for the BTES can be found in table 4.5.

When there is a heating demand, the BTES operates in the same way as for the base case, described in section 4.2.1. If the temperature requirement from section 4.3.1 is met, the PVTs will provide additional heat to the fluid before it enters the HP. When there is no heat demand but the prerequisite for the temperature in the PVT circuit is fulfilled, the BTES will be recharged. During the recharging, the direction of the circulation in the BHs will be reversed and heat is injected to the BHs.

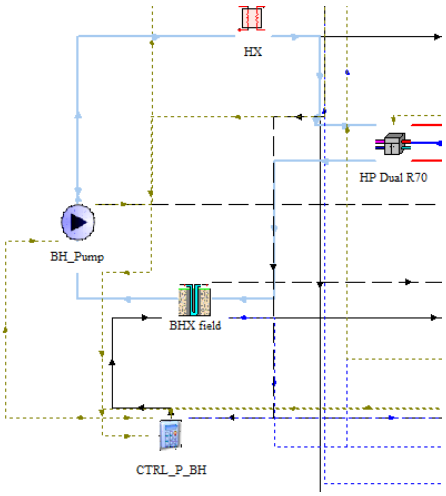


Figure 4.13: The BHE circuit in the TRNSYS model for model 2.

| Component | Parameter | Value | Unit |
|---|---|---|---|
| BHE field | | | |
| | Number of BHs | 8, 12, 16 | - |
| | Depth | 200 | $m$ |
| | Spacing | 20 | $m$ |
| Circulation pump | | | |
| | Maximum flow rate | 5 110 | $kg/hr$ |
| | Maximum power | 255 | $W$ |

Table 4.5: Main parameter values used for the BHE field for model 2.

### 4.3.3 Results

SAHPs gives the opportunity of reducing the volume of the BTES. To see how using solar technology together with the GSHP can reduce the size of the BHE field, the system has been simulated with a various number of BHs (8, 12 and 16) and a PVT collector of 100 $m^2$. The BHs have a distance of 20 m and a depth of 200 m. The simulations have been performed both over 1 year and 20 years, with a time-step of 2 minutes.

A large focus has been do improve the model to make it as reliable as possible, and to investigate how the system behaves. After running the simulations the first time, there was discovered a mistake in the model regarding the brine fluid's heat capacity.

The results from these simulations can be found in table B.1 in the appendix. A sensitivity analysis for the PVT collector area was also performed before the mistake was discovered. This can be seen in figure B.3 in appendix B.2.

Figure 4.14 shows the energy demands for different number of BHs with 100 $m^2$ of PVT. It can be seen that the energy consumption for auxiliary heating is decreasing with an increasing number of BHs, during the months with a SH demand. Evidently, the consumption varies with the ambient temperature. The coldest months are January, February and December, which is reflected in the chart. During the summer period, the consumption is similar for all alternatives, and it is covered by the electricity production from the PVT. From October to April, the energy used for pumps is almost twice as high for the base case compared to the system with a GSHP and PVT. This is because the simulation model for the base case provided by the co-supervisor has a twice as high maximum power for the pump in the BH circuit. Due to a lack of time, the simulations could not be re-run, but compared to the energy used for SH and the HP, the consumption is rather small and it is therefore assumed that the effect of it on the performance of model 1 is minimal.

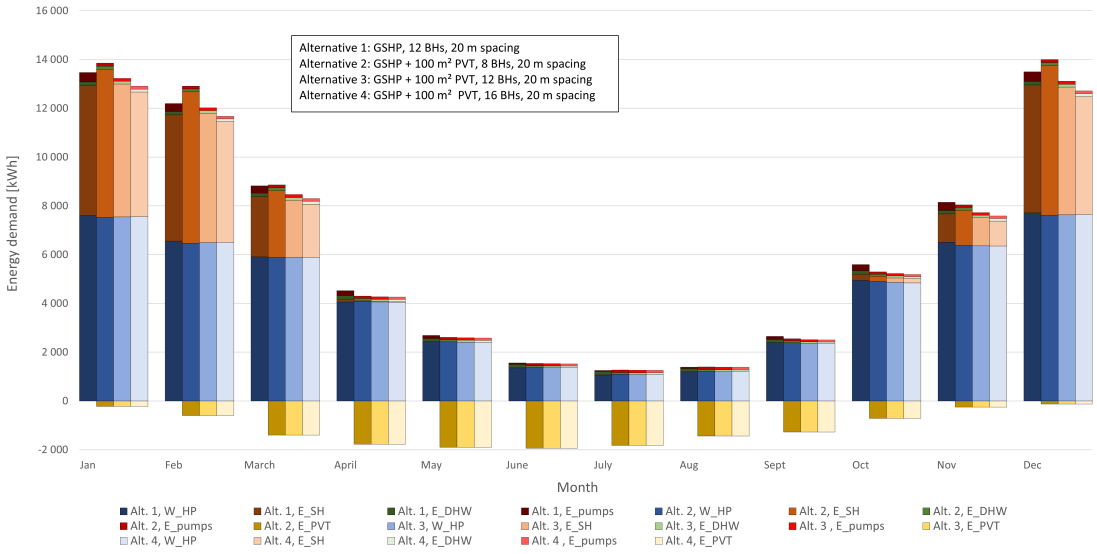


Figure 4.14: Comparison of the energy consumption with regards to the number of BHs in year 1.

The heat balance of the system with different number of BHs and the average brine temperature for year 1 can be seen in figure 4.15. A negative heat flow is in this

context defined as a heat gain to the system. There is not a balance between injection and extraction for any alternative. This could be because it is the first year of operation and a balance has not been established yet, or it could be because 100 $m^2$ of PVT is not adequate to compensate for the extraction. The average brine temperature is increasing with an increasing number of BHs.

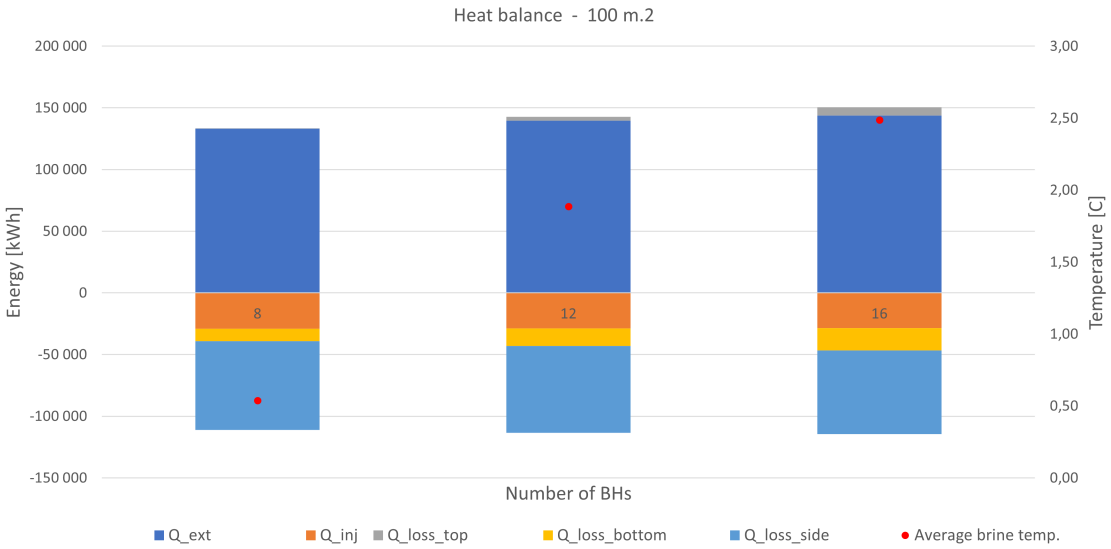


Figure 4.15: The heat balance and brine temperature the first year with 100 $m^2$ of PVT and different numbers of BHs.

Figure 4.16 shows the SPF and SPF4 for a GSHP with different numbers of BHs and 100 $m^2$ of PVT, and a stand-alone GSHP with 12 BHs for comparison. The variations throughout the year are similar to the results achieved for model 1, with the SPF4 being at its highest during the fall and spring, and SPF at its highest during the heating season. Adding 100 $m^2$ of PVT to a GSHP with 8 BHs is not sufficient to increase the KPIs enough to match a stand-alone GSHP with 12 BHs, except for in the summer months.

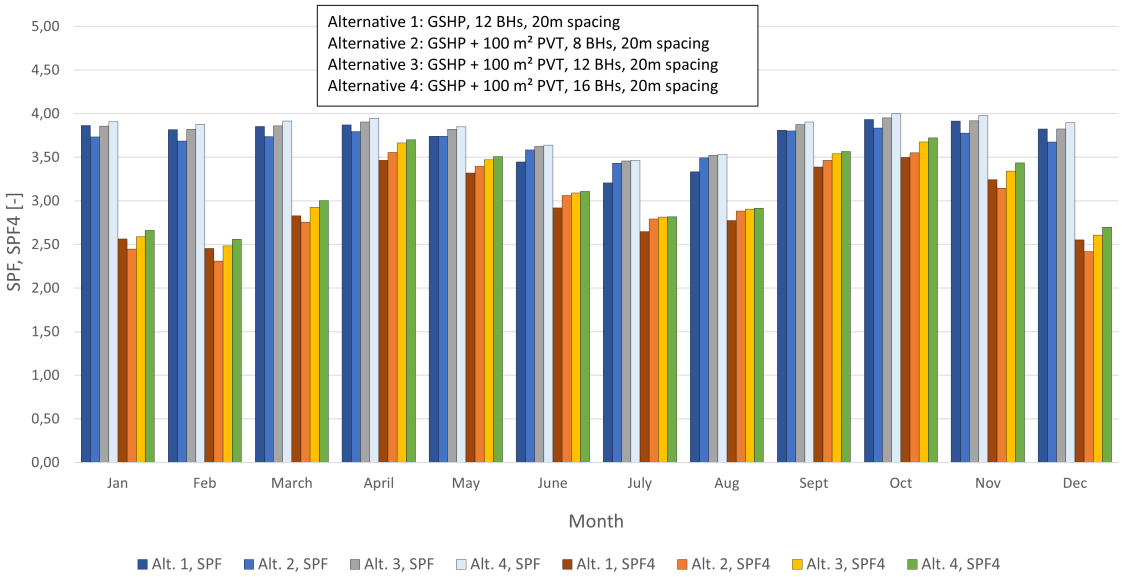


Figure 4.16: The SPF and SPF4 throughout the first year with 100 $m^2$ of PVT and different numbers of BHs.

**Long term results**

The main KPIs for the first year, after 20 years and the average over 20 year for the GSHP with 100 $m^2$ PVT can be seen in table 4.6. The minimum average fluid temperatures in the BHE are between 2.79 °C and -1.43 °C in year 20. While the average mean fluid temperatures are between 1.13 and 3.02. The alternative with 8 BHs achieves the lowest 20-year average fluid temperature.

Figure 4.17 shows the progression of the SPF and SPF4 for all the alternatives of BHs over 20 years. The reduction in SPF and SPF4 from year 1 to year 20 is around 2.5-4.0 % and 4.5-6.5%. The heat injected from the PVT is insufficient to establish a balance between injection and extraction. As the number of BHs decreases, the KPIs are progressively reduced over the years due to less available heat and reduced heat gains from the surrounding ground caused by a smaller surface area. Increasing the number of BHs from 8 to 12, leads to a rise in the SPF and SPF4 of 3.6% and 6.6% in year 20. Further on, doubling from 8 to 16 BHs leads to an ascend of the SPF and SPF4 of 6.1 % and 10.5 %, respectively. The reason for this is that a higher amount of heat is extracted from the BTES with more BHs. For the same reason, the regeneration fraction is at its lowest with 16 BHs, with only 20% in year 20. The increase in the regeneration fraction over the years is due to an increased thermal

production in the PVT. The mean SPF4 over 20 years for 8, 12 and 16 BHs is 2.64, 2.81 and 2.91, respectively.

From the communication with Gilbert Jensen on the 18th of April 2023, the SPF4 for a system with GSHP and PVT should be above 3 and the SPF should increase by 25-50%. In addition, the typical PVT-GSHP ratio is 1-1.5 $m^2$ PVT uninsulated panels/kW HP. For this system that results in approximately 70-100 $m^2$ PVT panels. From table 4.6 it can be seen that the SPF4 is below 3 for all alternatives, besides in year 1 with 16 BHs. In addition, adding 100 $m^2$ of PVT to a GSHP with 12 BHs only improves the SPF with 0.52% in year 1 and 1.64% in year 20. From the conversation with Gilbert, a possible reason for not achieving better results could be the control algorithms that are implemented.

| Number of BHs | Year | SPF [-] | SPF4 [-] | $Reg_{frac}$ [-] | Minimum $T_m$ [° C] |
|---|---|---|---|---|---|
| 8 | 1 | 3.73 | 2.76 | 0.18 | 0.29 |
| | 20 | 3.58 | 2.58 | 0.23 | -1.43 |
| | Avg. | 3.63 | 2.64 | 0.20 | 1.13 |
| 12 | 1 | 3.84 | 2.92 | 0.17 | 2.04 |
| | 20 | 3.71 | 2.75 | 0.21 | 0.36 |
| | Avg. | 3.76 | 2.81 | 0.19 | 2.46 |
| 16 | 1 | 3.90 | 2.99 | 0.17 | 2.69 |
| | 20 | 3.80 | 2.85 | 0.20 | 1.16 |
| | Avg. | 3.84 | 2.91 | 0.19 | 3.02 |

Table 4.6: Summary of the KPIs for the GSHP with 100 $m^2$ PVT over 20 years.

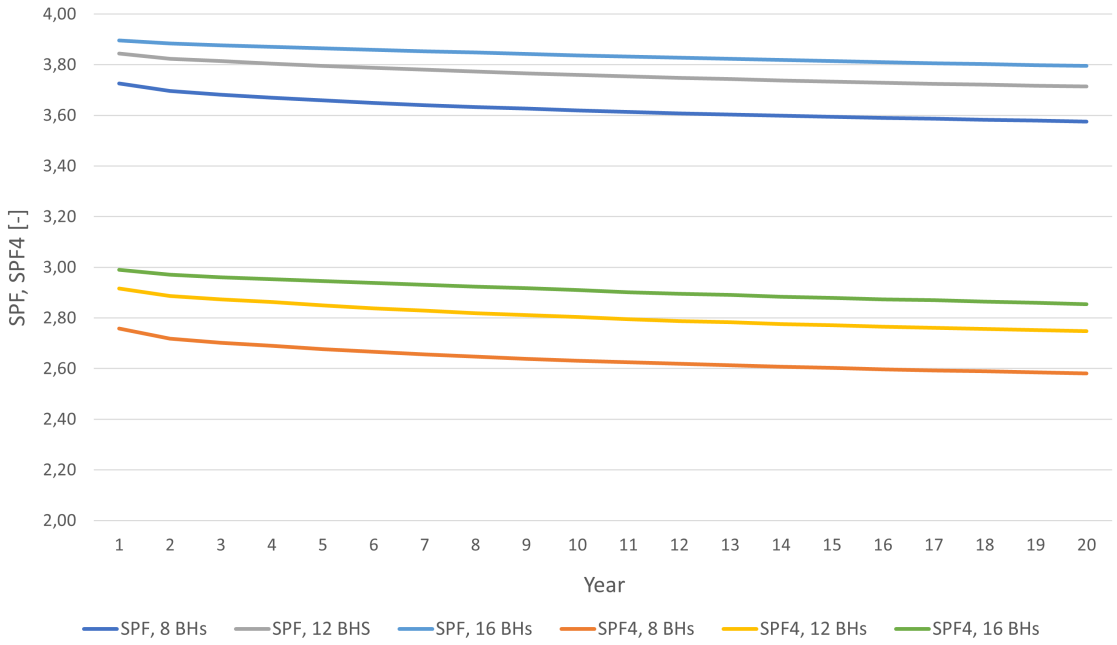


Figure 4.17: Comparison of the SPF and SPF4 for model 2.

The average brine fluid temperature for a GSHP with 12 BHs with 100 $m^2$ of PVT is illustrated in figure 4.18. The oscillations are caused by the heat extraction during the winter and the injection during the summer. After 20 years it is still decreasing and has not yet reached a steady-state.

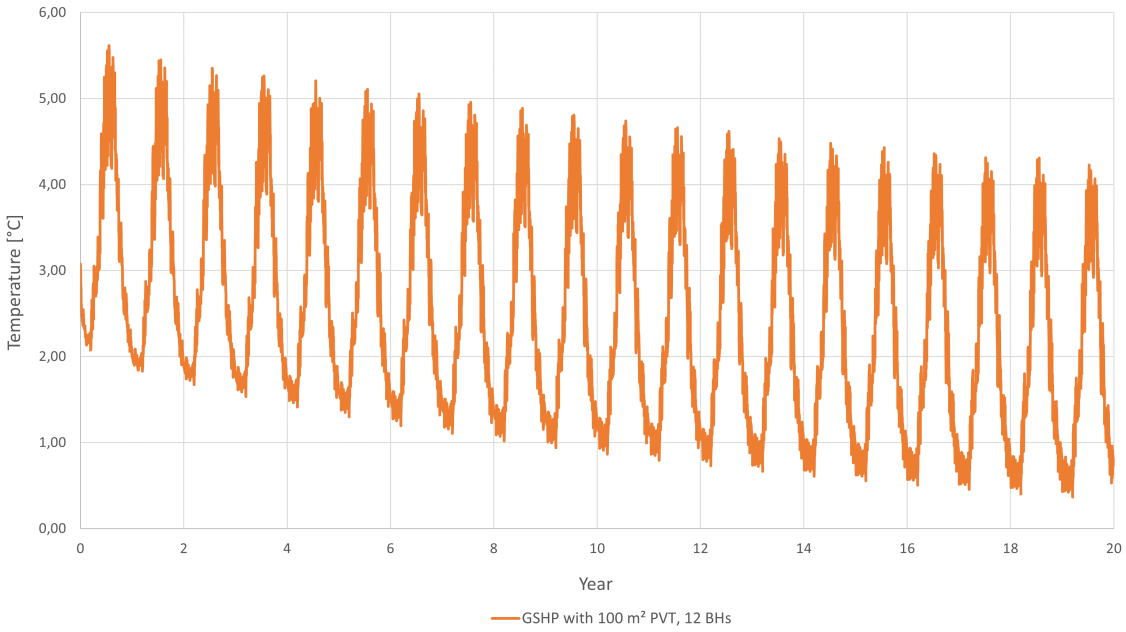


Figure 4.18: Average brine fluid temperature for the GSHP system with 12 BHs and 100 $m^2$ of PVT over the first 20 years.

### 4.3.4 Effect of increasing the PVT area

The effect on the performance by increasing the PVT area has been investigated for three sizes of PVT: 100 $m^2$, 200 $m^2$ and 300 $m^2$. It has been simulated for 8, 12 and 16 BHs with a spacing of 20 m and a depth of 200 m.

An illustration of how the SPF, SPF4 and regeneration fractions varies for the different variants of BHs and PVT area are illustrated in figure 4.19. The increase in SPF and SPF4 by adding more PVT is rather small, whilst the regeneration fraction goes from around 20%, with 100 $m^2$ of PVT, to above 40% with 300 $m^2$ of PVT.

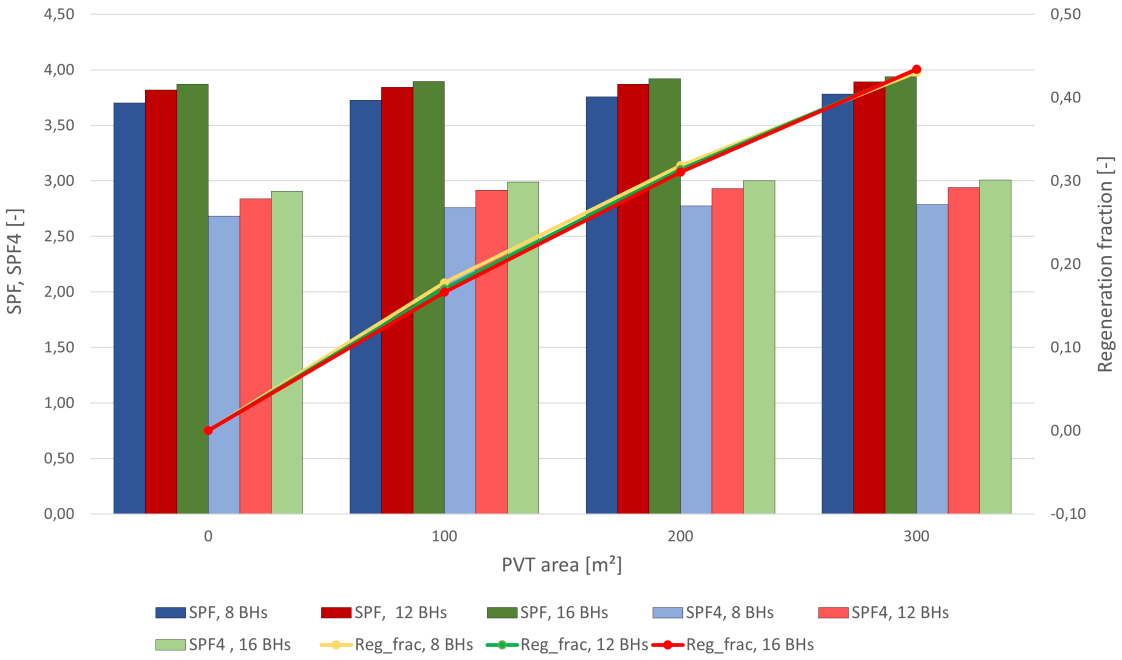


Figure 4.19: Comparison of the SPF and SPF4 with regards to the area of PVT in year 1.

By adding more and more PVT, it would be expected that the auxiliary heating for SH would decrease due to more extracted heat. From figure 4.20, this is not the case. From the communication with Gilbert Jensen on the 18th of April 2023, it is clear that the energy for peak load should be reduced by 6-100%. After consulting with the supervisors, it is still difficult to conclude why this is not happening, but a plausible answer could be that the HP power coverage is too low. It can also be seen in figure 4.21 that the heat extracted is approximately the same for all cases with 8 BHs, but the temperature is increasing. Additionally, there is not a balance in the gains and losses, which could indicate that the amount of injected heat is too low.

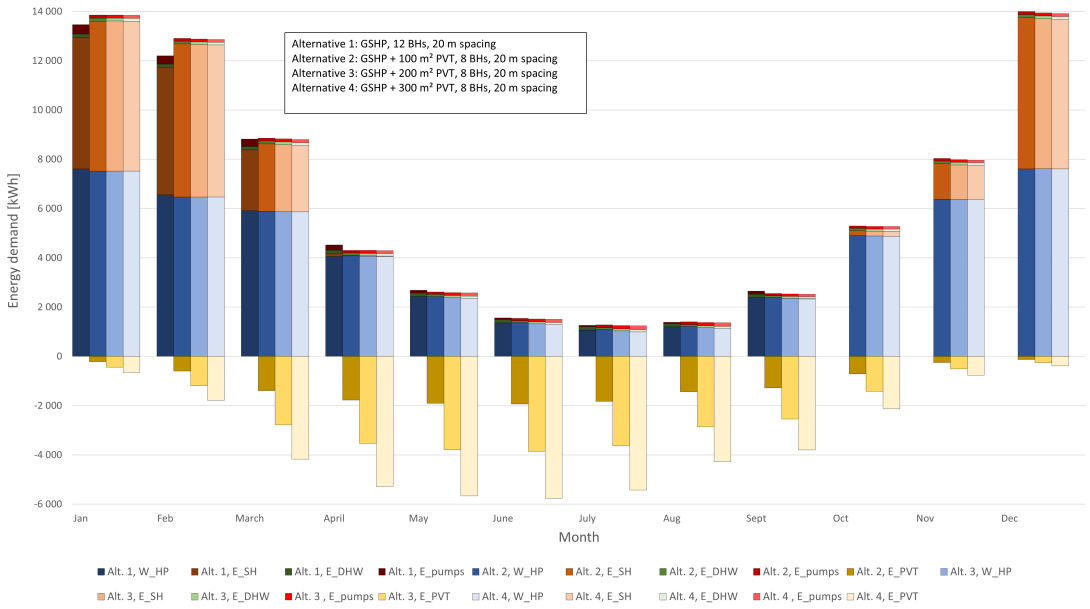


Figure 4.20: Comparison of the energy consumption the first year with regards to the area of PVT in model 2 with 8 BHs.

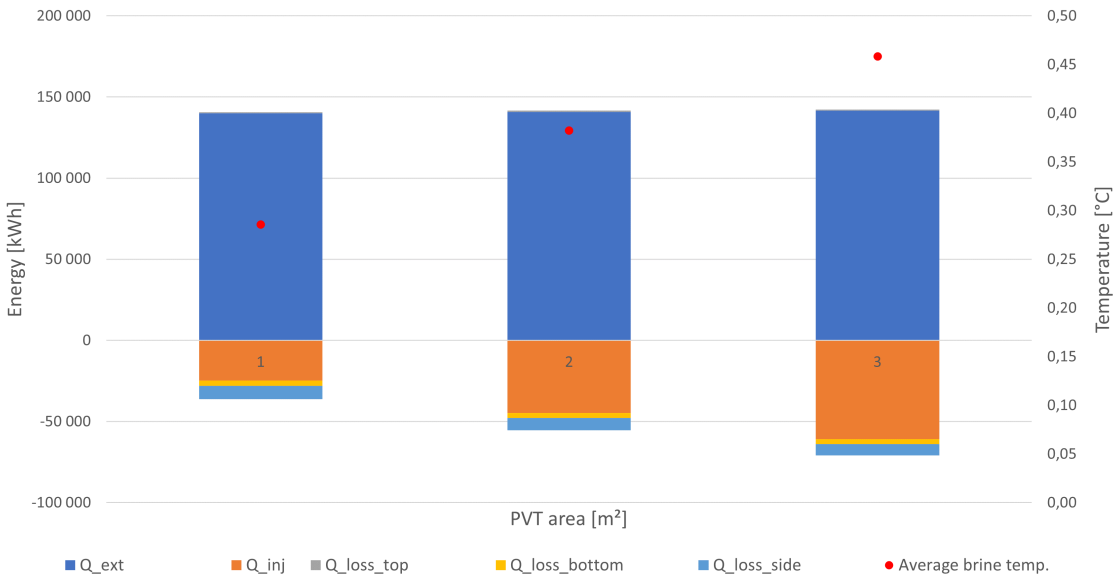


Figure 4.21: The heat balance and brine temperature the first year with 8 BHs and different sizes of PVT.

The main KPIs for the first year and after 20 years can be seen in table 4.7. The minimum average fluid temperatures in the BHE field are between 2.79 °C and -1.43 °C in year 20. The alternative of a GSHP and PVT with 8 BHs achieves the lowest minimum average fluid temperature in year 20 for all the PVT areas.

With a doubling in the collector area from 100 $m^2$ to 200 $m^2$ with 12 BHs, SPF and SPF4 in year 20 is increased by 1.9% and 1.8%. These improvements are insignificant. Tripling the PVT collector area from 100 $m^2$ to 300 $m^2$ increases the SPF and SPF4 by 3.0% and 2.5%, respectively. Adding 300 $m^2$ of PVT to a GSHP system with 12 BHs increases the SPF by 1.83% in year 1 and 4.66% in year 20. This is lower than what is achieved by N. Sommerfeldt and H. Madani [35], but a reason could be differences in the system design.

From the results, it appears that increasing the number of BHs has a bigger impact on SPF and SPF4 than the area of PVT, as doubling from 8 to 16 BHs leads to an ascend of 6.1 % and 10.5 %, with 100 $m^2$ of PVT. The reason for this is that a higher amount of heat is extracted from the BTES with more BHs.

The regeneration fraction varies from 18% to 49 %, depending on the PVT collector area, and is at its highest with 300 $m^2$. The number of BHs does not have a big impact, due to approximately the same amount of heat being extracted and injected regardless.

| PVT collector area [m$^2$] | Number of boreholes | Year | SPF [-] | SPF4 [-] | $Reg_{frac}$ [-] | Minimum $T_m$ [° C] |
|---|---|---|---|---|---|---|
| 100 | 8 | 1 | 3.73 | 2.76 | 0.18 | 0.29 |
| | | 20 | 3.58 | 2.58 | 0.23 | -1.43 |
| | 12 | 1 | 3.84 | 2.92 | 0.17 | 2.04 |
| | | 20 | 3.71 | 2.75 | 0.21 | 0.36 |
| | 16 | 1 | 3.90 | 2.99 | 0.17 | 2.69 |
| | | 20 | 3.80 | 2.85 | 0.20 | 1.16 |
| 200 | 8 | 1 | 3.76 | 2.77 | 0.32 | 0.38 |
| | | 20 | 3.64 | 2.64 | 0.38 | -1.00 |
| | 12 | 1 | 3.87 | 2.93 | 0.31 | 2.11 |
| | | 20 | 3.78 | 2.80 | 0.37 | 0.77 |
| | 16 | 1 | 3.92 | 3.00 | 0.31 | 2.76 |
| | | 20 | 3.85 | 2.90 | 0.36 | 1.48 |
| 300 | 8 | 1 | 3.78 | 2.79 | 0.43 | 0.46 |
| | | 20 | 3.70 | 2.68 | 0.49 | -0.67 |
| | 12 | 1 | 3.89 | 2.94 | 0.43 | 2.14 |
| | | 20 | 3.82 | 2.84 | 0.49 | 1.09 |
| | 16 | 1 | 3.94 | 3.01 | 0.43 | 2.79 |
| | | 20 | 3.89 | 2.94 | 0.49 | 1.75 |

Table 4.7: Summary of the KPIs for the GSHP with different areas of PVT over 20 years.

### 4.3.5 Effect of reducing the borehole spacing

An advantage of adding solar technology is the possibility to reduce the size of the BH field. A prerequisite for this is that there is a somewhat balance between injection and rejection of heat. To investigate if this is possible for this system, the spacing has been reduced from 20 m to 10 m.

The KPIs achieved from the simulations of a GSHP with 100 m $^2$ with a BH spacing of 20 m and 10 m is summarized in table 4.8. The results shows that for all numbers of BHs, the SPF and SPF4 are reduced with a smaller spacing. This is especially prominent in year 20. The minimum average brine fluid temperature is also reduced significantly, from -1.43 °C to -2.38 °C for 8 BHs in year 20.

| Spacing [$m$] | Number of BHs | Year | SPF [-] | SPF4 [-] | $Reg_{frac}$ [-] | Minimum $T_m$ [° C] |
|---|---|---|---|---|---|---|
| 10 | 8 | 1 | 3.72 | 2.75 | 0.18 | 0.09 |
| | | 20 | 3.50 | 2.50 | 0.25 | -2.38 |
| | 12 | 1 | 3.84 | 2.91 | 0.17 | 1.87 |
| | | 20 | 3.62 | 2.64 | 0.24 | -0.81 |
| | 16 | 1 | 3.89 | 2.99 | 0.17 | 2.52 |
| | | 20 | 3.70 | 2.74 | 0.23 | -0.04 |
| 20 | 8 | 1 | 3.73 | 2.76 | 0.18 | 0.29 |
| | | 20 | 3.58 | 2.58 | 0.23 | -1.43 |
| | 12 | 1 | 3.84 | 2.92 | 0.17 | 2.04 |
| | | 20 | 3.71 | 2.75 | 0.21 | 0.36 |
| | 16 | 1 | 3.90 | 2.99 | 0.17 | 2.69 |
| | | 20 | 3.80 | 2.85 | 0.20 | 1.16 |

Table 4.8: KPIs for a GSHP with 100 $m^2$ PVT with a BH spacing of 20 m and 10 m.

The average storage temperatures with a spacing of 20 m and 10 m are illustrated in figure 4.22. The temperature with 10 m spacing is significantly lower and reduced faster than with 20 m spacing. After discussions with the supervisors, a possible reason could be that the amount of heat injected from the PVT is not sufficient enough to justify reducing the surface area. A paper from Skarphagen et al. [26] supports this assumption.

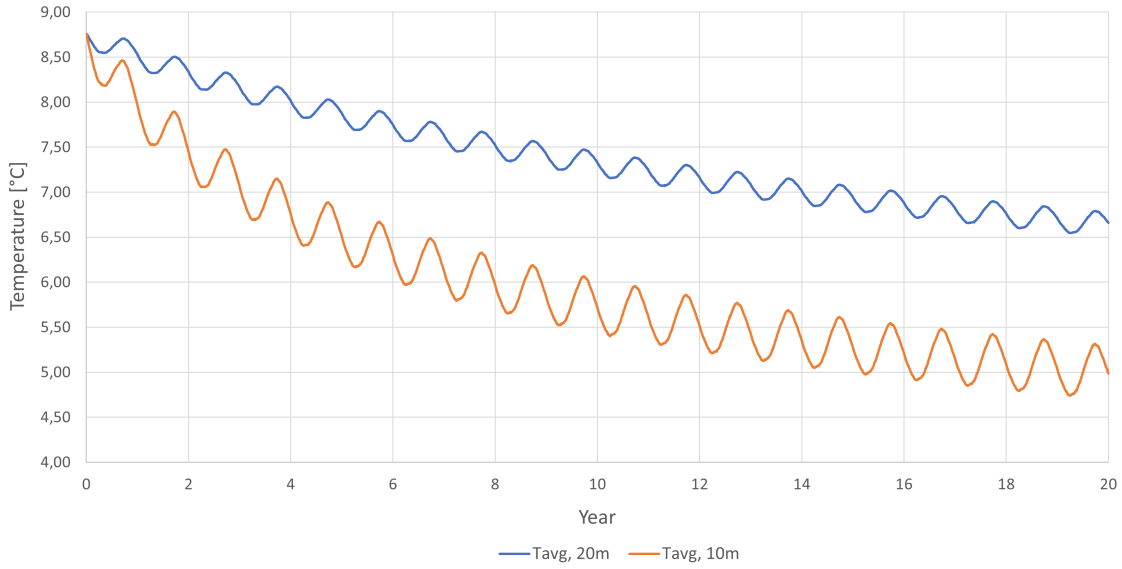


Figure 4.22: The average storage temperature for option 1 and option 2 with 12 BHs and 100 $m^2$ PVT.

### 4.3.6 Effect of increasing the power coverage factor

In section 4.3.4, it was discovered that adding more PVT did not decrease of energy consumption for SH. After discussing it with the supervisors, a possible solution could be to increase the power coverage factor of the HP. Simulations with a power coverage factor of 80% and 90% have thus been carried out, in addition to the ones with 70% coverage.

The delivered energy with 80 and 90% power coverage with 12 BHs and different sizes of PVT, compared to 70% coverage can be seen in figures 4.23 and 4.24. It can be seen that even with a higher power coverage factor, the delivered energy for SH is still not decreasing with an increasing PVT area. However, it does reduce the energy consumption compared to 70% power coverage, as expected.

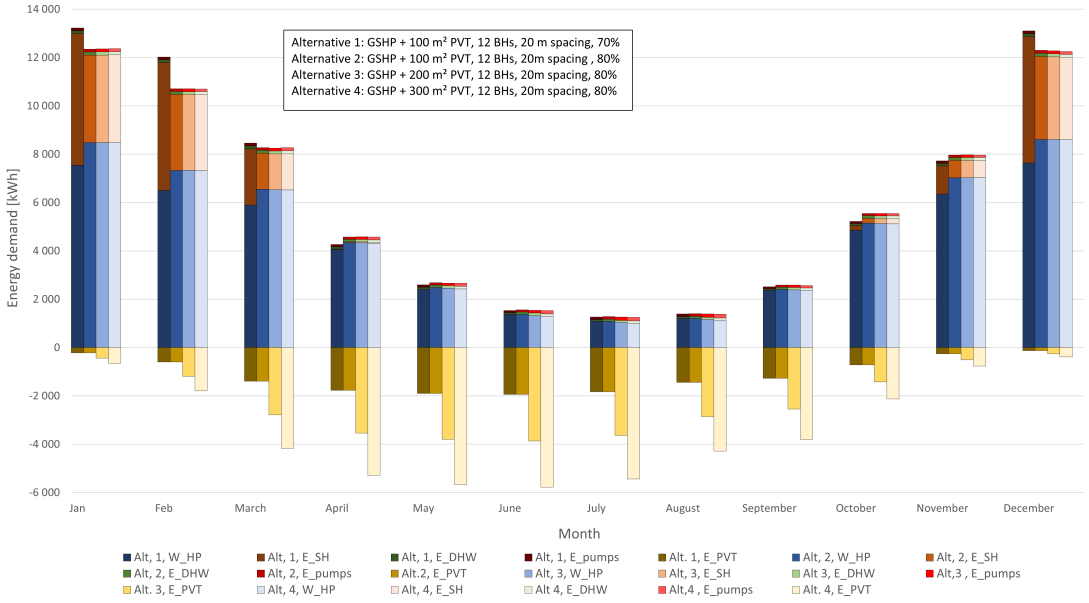


Figure 4.23: Comparison of the energy consumption the first year with different PVT collector areas with a power coverage factor of 80% for a GSHP with 12 BHs.

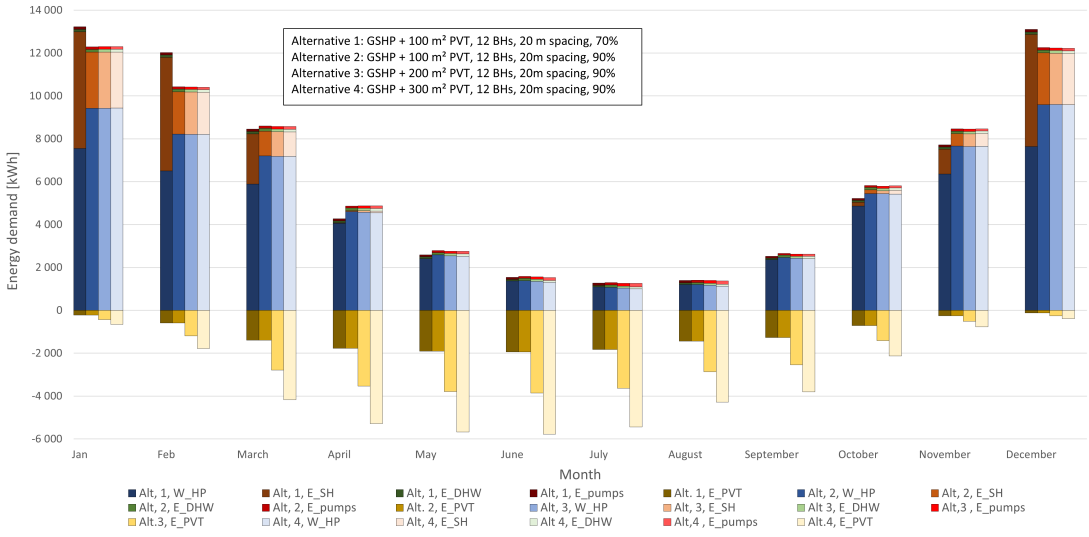


Figure 4.24: Comparison of the energy consumption the first year with different PVT collector areas with a power coverage factor of 90% for a GSHP with 12 BHs.

Figure 4.25 shows that the biggest difference seem to be by increasing the power coverage from 70% to 80%, especially in the coldest months. Another interesting thing is that during the month where a medium auxiliary SH demand is present, like in November, March and April, the energy consumption is higher for the solution with a 90% coverage. The reason for this is that the HP only has the possibility to operate at full effect, which with a small heat load causes it to turn on and off more rapidly. This increases the energy consumption and the wear and tear of the HP.

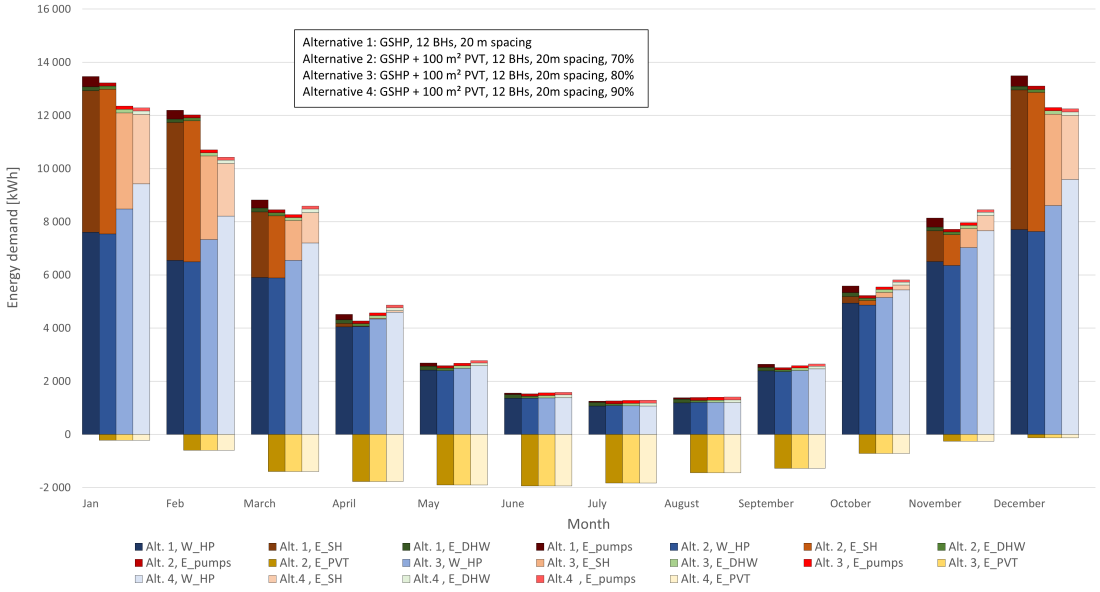


Figure 4.25: Comparison of the energy consumption the first year with different power coverage factors for a GSHP with 12 BHs and 100 $m^2$ of PVT.

The SPF and SPF4 over 20 years for the different power coverage factors for a GSHP with 12 BHs and 100 $m^2$ of PVT can be seen in figure 4.26. The SPF is nearly the same for all alternatives, but slightly more reduced by year 20 for 80% and 90%. This is due to a higher heat extraction during the first years of operation, which leads to a higher decrease in the temperature over the years and therefore a bigger reduction in extracted energy over 20 years. It can also be seen that a higher power coverage factor leads to a higher SPF4, due to the lower energy consumption of the system. In table 4.9, the main KPIs are summarized for all three alternatives of power coverage for a GSHP with 100 $m^2$ of PVT. Increasing the coverage factor from 70 to 90% leads to a decrease in the temperature from -1.43°C to -3.61 °C with 8 BHs in year

20. For both 80 and 90% power coverage, the SPF4 is above 3, except for in year 20 with 8 BHs.

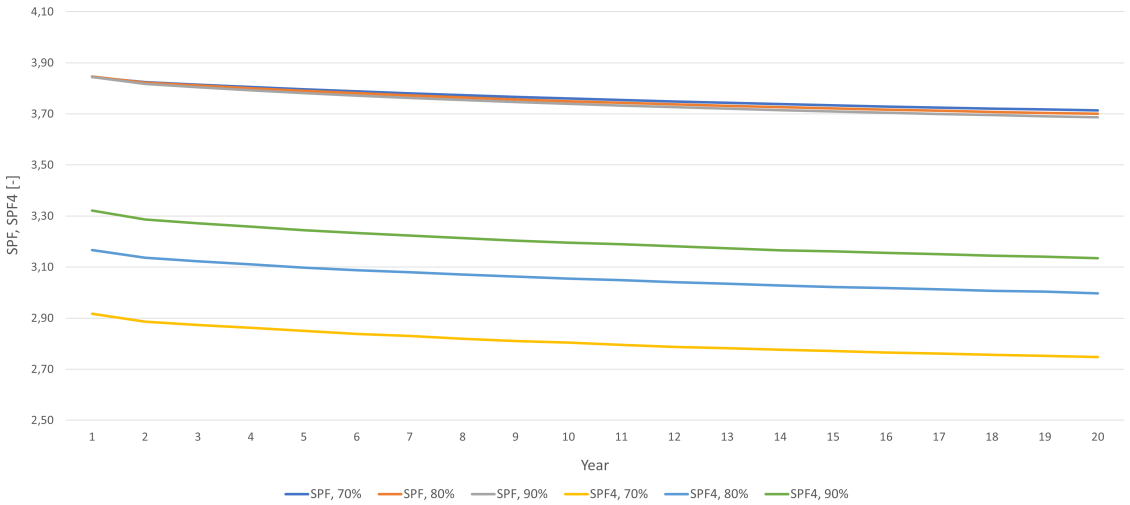


Figure 4.26: Comparison of the SPF and SPF4 with different power coverage factors for a GSHP with 12 BHs and 100 $m^2$ of PVT.

| Power Coverage [%] | Number of BHs | Year | SPF [-] | SPF4 [-] | Minimum $T_m$ [° C] |
|---|---|---|---|---|---|
| 70 | 8 | 1 | 3.73 | 2.76 | 0.29 |
| | | 20 | 3.58 | 2.58 | -1.43 |
| | 12 | 1 | 3.84 | 2.92 | 2.04 |
| | | 20 | 3.71 | 2.75 | 0.36 |
| | 16 | 1 | 3.90 | 2.99 | 2.69 |
| | | 20 | 3.80 | 2.85 | 1.16 |
| 80 | 8 | 1 | 4.71 | 3.01 | -0.71 |
| | | 20 | 3.55 | 2.80 | -2.55 |
| | 12 | 1 | 3.85 | 3.17 | 1.20 |
| | | 20 | 3.70 | 3.00 | -0.66 |
| | 16 | 1 | 3.91 | 3.24 | 1.87 |
| | | 20 | 3.79 | 3.10 | 0.24 |
| 90 | 8 | 1 | 3.70 | 3.15 | -1.66 |
| | | 20 | 3.52 | 2.94 | -3.61 |
| | 12 | 1 | 3.84 | 3.32 | 0.35 |
| | | 20 | 3.69 | 3.14 | -1.60 |
| | 16 | 1 | 3.91 | 3.40 | 1.08 |
| | | 20 | 3.78 | 3.25 | -0.67 |

Table 4.9: Results of increasing the power coverage for the GSHP with 100 $m^2$ PVT.

## 4.4 Model 3: Photovoltaic panel

The simulation of PV production can be done separately, and the load and GSHP circuit is therefore not needed. The TRNSYS component used for the PV (Type 562d) is described in section 3.4.2, and the parameters that have been changed are summarized in table 4.10. The model in TRNSYS can be seen in figure 4.27. The weather conditions are the same as described in section 3.1.

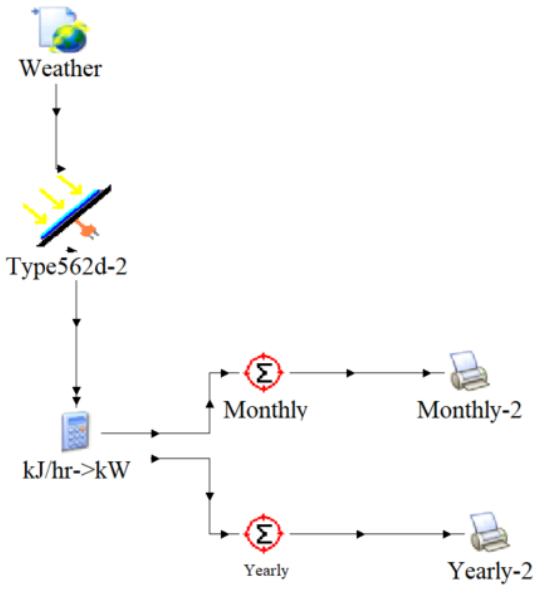


Figure 4.27: The PV model in TRNSYS.

| Parameter | Value | Unit |
|---|---|---|
| Area | 100, 200, 300 | $[m^2]$ |
| Reference PV efficiency | 20.4 | [%] |
| Reference temperature | 25 | $[°C]$ |
| Reference radiation | 1000 | $[W/m^2]$ |
| Cover thickness | 32 | $[mm]$ |
| Slope | 44 | ° |

Table 4.10: Input values used for the PVT in TRNSYS [55].

### 4.4.1 Results

The system has been simulated for 1 year, with a simulation step of 2 minutes. It has been simulated with three sizes of PV: 100, 200 and 300 $m^2$.

The production from the different sized PV systems can be seen in figure 4.28. During the coldest months November, October and December, the production is at its lowest. It peaks during the summer months.

The total yearly production is summarized in table 4.11. The produced energy increases linearly with the increased area of the PV field, and doubling the area

results in a doubling of the produced energy. According to the Norwegian Water Resources and Energy Directorate, a PV facility in Norway will produce between 650 and 1 000 kwh/kWp. With a production of 753 kWh/kWp achieved for this facility, the results seem reasonable.

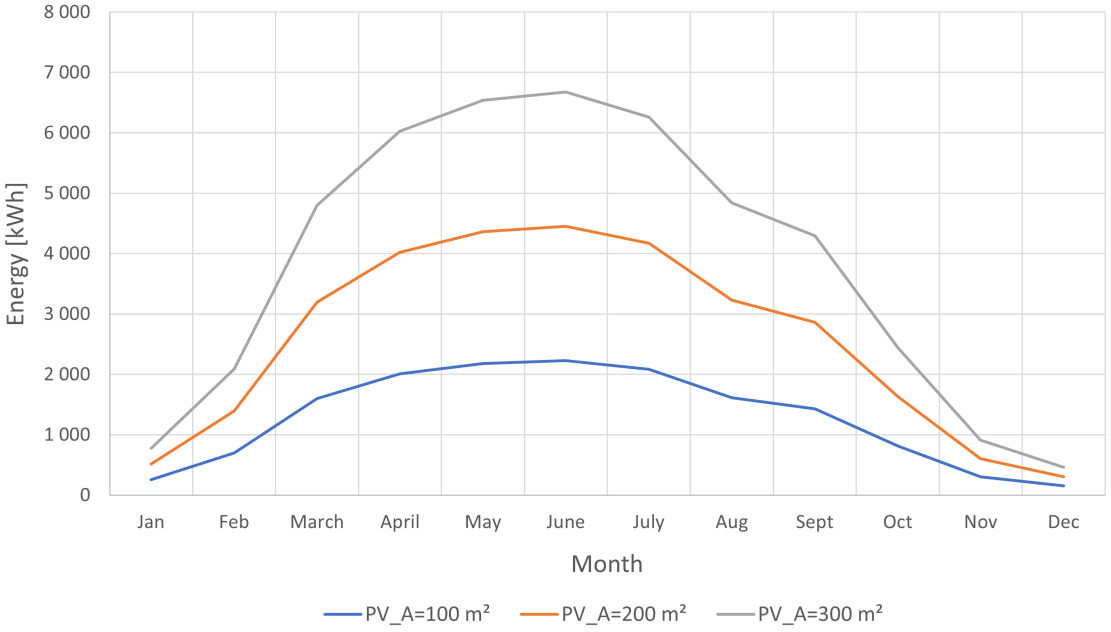


Figure 4.28: Production from the PV with areas of 100, 200 and 300 $m^2$.

| PV area [$m^2$] | kWp | Production [kWh] | Production [kWh/kWp] |
|---|---|---|---|
| 100 | 20.4 | 15 369 | 753.4 |
| 200 | 40.8 | 30 738 | 753.4 |
| 300 | 61.2 | 48 108 | 753.4 |

Table 4.11: Yearly PV production for the different PV sizes.

# 5 Comparison

In this section, the three models presented in sections 4.2, 4.3 and 4.4 will be compared. To compare the different systems, the KPIs from section 4.1 will be used in addition to the energy production in the PV and PVT. By adding PVT, the goal is to be able to reduce the number of BHs. According to the supervisor, it should be possible to reduce the number by around 10-20%. In this thesis, the systems have been simulated with 8, 12 and 16 BHs, and the only option is to reduce it by 4 BHs. Results found in section 4.3.4 showed that the effect of increasing the PVT area is minimal, and PVT and PV areas of 100 $m^2$ will therefore be used. The alternatives will be compared with the parameters found in table 5.1. For the alternative with PV, the gross energy consumption and energy flows are the same as for the stand-alone GSHP. The four alternatives compared are:

- Alternative 1: GSHP, 12 BHs, 20 m spacing
- Alternative 2: GSHP + 100 $m^2$ PVT, 8 BHs, 20m spacing
- Alternative 3: GSHP + 100 $m^2$ PVT, 12 BHs, 20m spacing
- Alternative 4: GSHP + 100 $m^2$ PV, 12 BHs, 20m spacing

| Parameter | Value | Unit |
|---|---|---|
| Spacing | 20 | $m$ |
| Depth | 200 | $m$ |
| Power coverage factor | 0.7 | - |
| PV/PVT area | 100 | $m^2$ |

Table 5.1: Parameters that are common for all alternatives compared.

## 5.1 Electricity production

From figure 5.1 it can be seen that the electricity production is higher with PV than PVT. The heat extraction in the PVT should increase the electricity production by 10-15% per year. The difference is likely due to the difference in efficiency of the PV and PVT. The PV has an efficiency of 20.4% while the PVT has a PV efficiency of only 17.0 %.

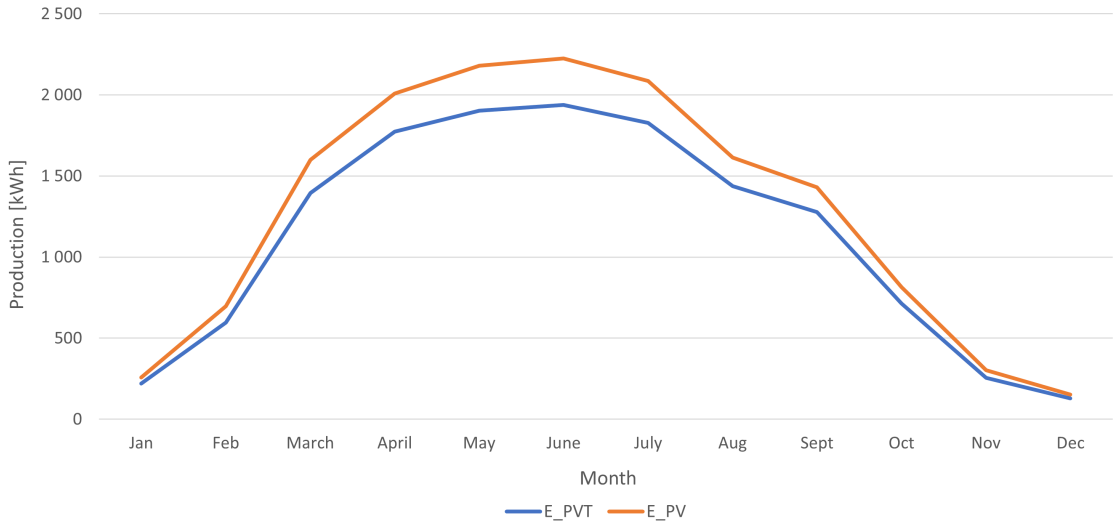


Figure 5.1: Comparison of production of electricity with PV and PVT over the first year of operation.

## 5.2 Key performance indicators

This section contains a comparison of the KPIs for the different alternatives of the models. Since none of the KPIs presented in this thesis takes electricity produced on-site into consideration, the performance indicators for alternative 1 (only GSHP) and 4 (GSHP + PV) will be the same.

### 5.2.1 SPF

SPFs during the first year of operation are shown in figure 5.2. When the heat demand is at its highest during the winter months, the stand-alone GSHP with and without PV achieves a higher SPF than alternative 2. This is likely because 100 $m^2$ of PVT does not recharge the BHs sufficient to cover the reduction in BHs. During the summertime, the PVT increases the performance due to a heating demand mostly consisting of only high-temperature DHW and a higher average brine fluid temperature in the BHE field. Alternative 3 with 12 BHs and 100 $m^2$ of PVT achieves the highest SPF for all months.

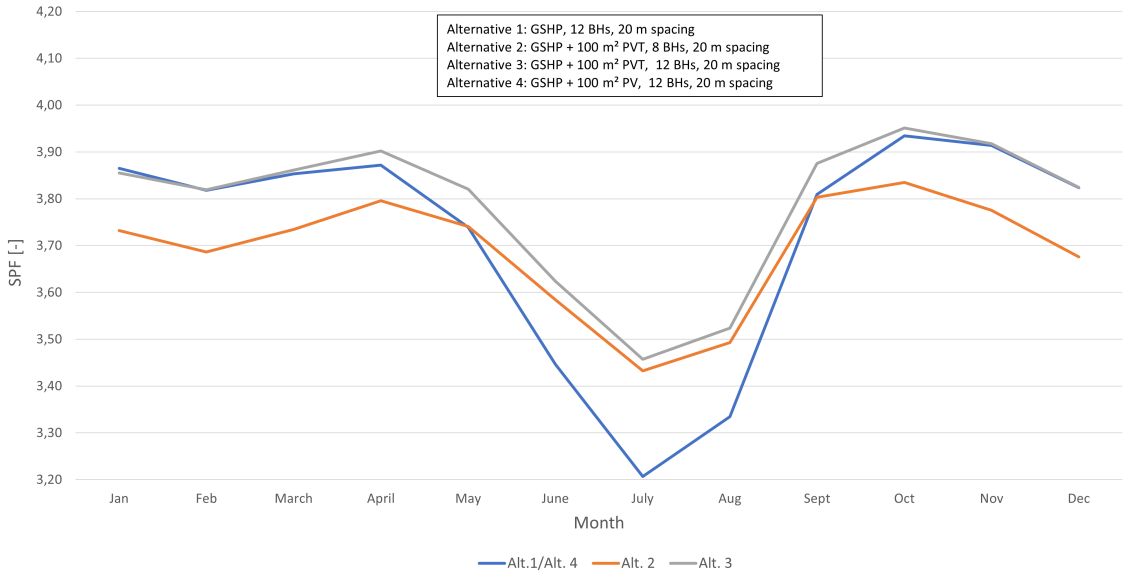


Figure 5.2: Comparison of SPF for the alternatives during the first year of operation.

Figure 5.3 shows the SPF for all alternatives over 20 years. The decrease of SPF for the GSHP is 4.5%, whereas for the PVT-SAHP alternatives 2 and 3 it is 4.0% and 3.4%, respectively. Additionally, adding 100 $m^2$ of PVT to a GSHP with 12 BHs increases the SPF by 1.6% in year 20. With only 20 years as the simulation period the SPF is still decreasing at the end of the analysis for all alternatives. Reducing the BH number for the PVT-SAHP from 12 to 8 leads to a decrease of the SPF of 2.9% in year 1, and 3.5 % in year 20.

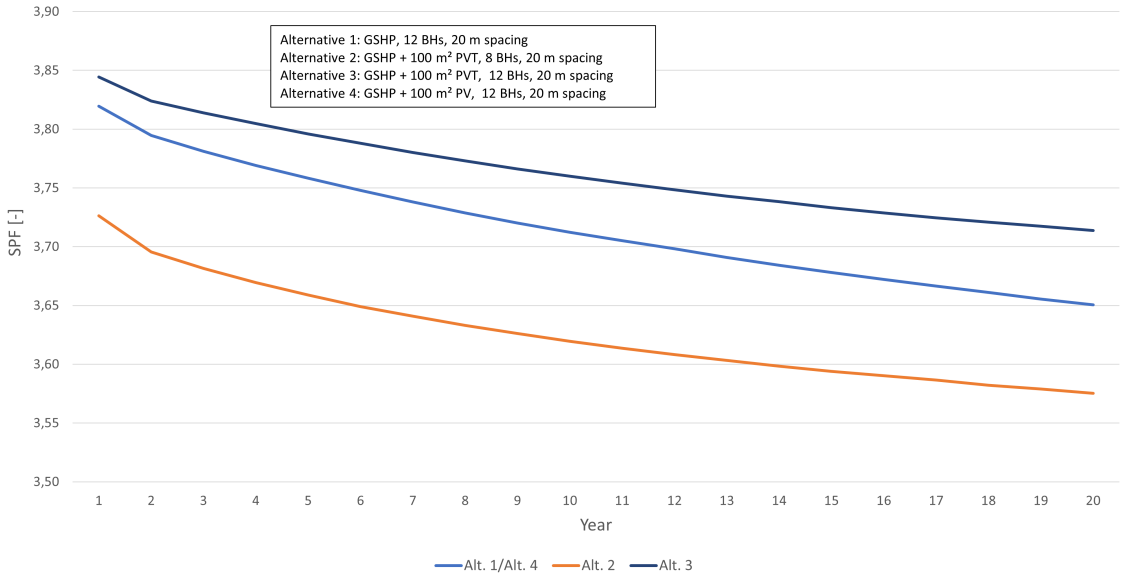


Figure 5.3: Comparison of SPF for the alternatives over 20 years of operation.

### 5.2.2 SPF4

The SPF4 is more even throughout the first year for all alternatives than SPF, as can be seen in figure 5.4. As with the SPF, it is higher for alternative 1 and 4 in the winter period than for alternative 2, and lower in the summer months. It is at its highest for alternative 3 all year.

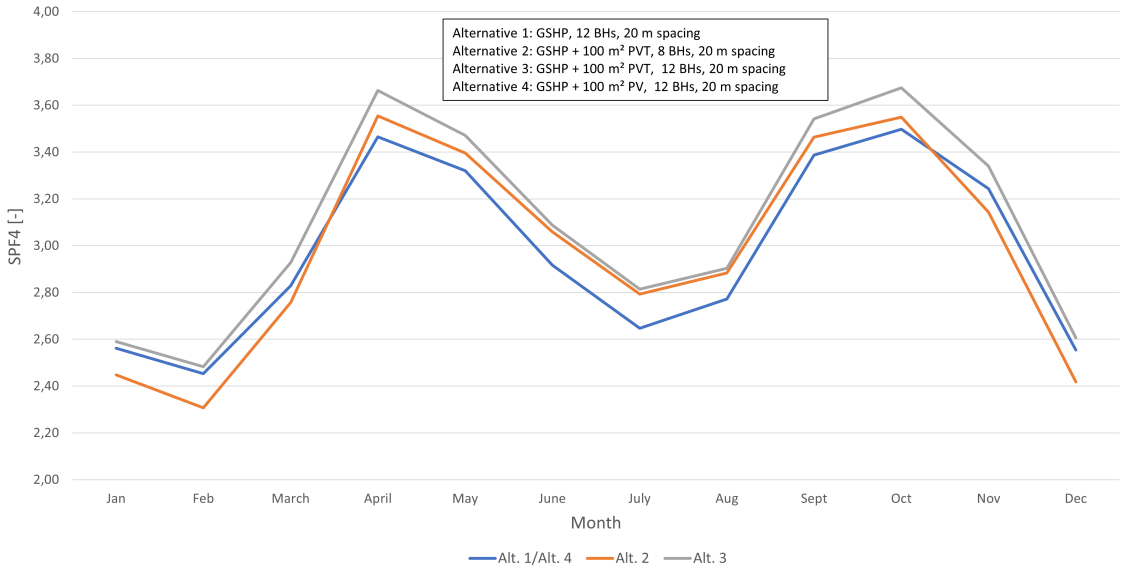


Figure 5.4: Comparison of SPF4 for the alternatives during the first year of operation.

The SPF4 over 20 years is illustrated in figure 5.5. The decrease over time is more steep for alternatives 1 and 4, with a decrease of 7.4% over 20 years. For alternative 2 and 3, it is 6.5% and 5.8%, respectively. Alternative 1 and 4 outperforms alternative 2 with reduced number of BHs. In this work, a relatively large reduction of BHs has been used, and it could be that a decrease of 2 BHs instead of 4 would be more in favor for the PVT system.

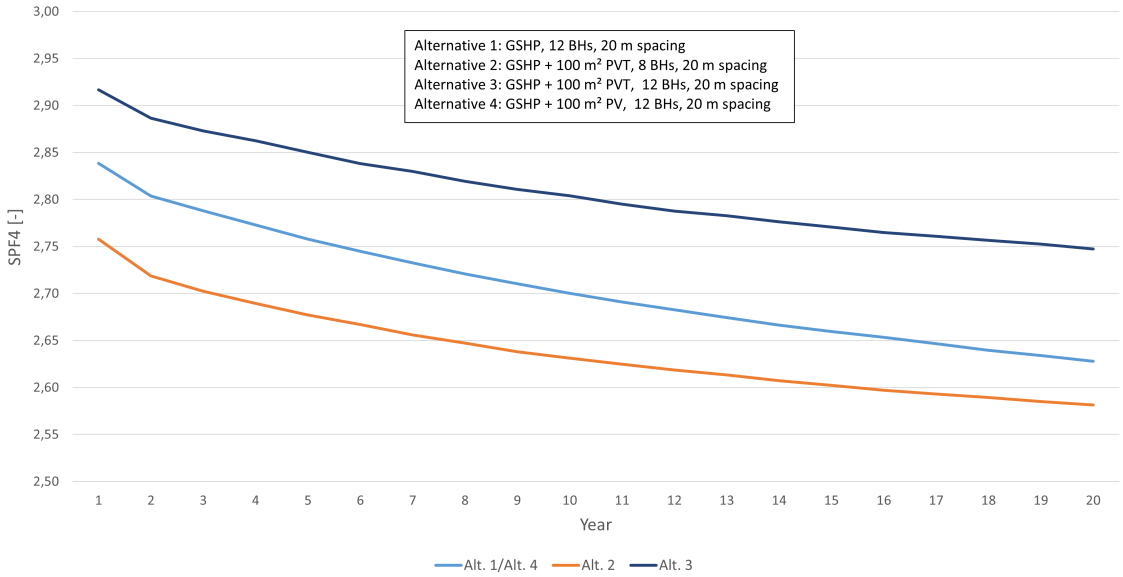


Figure 5.5: Comparison of SPF4 for the alternatives over 20 years of operation.

### 5.2.3 Average brine fluid temperature

The average brine fluid temperatures for the four alternatives are illustrated in figure 5.6. The first years of operation, the lows during the winter are similar for alternative 1, 3 and 4. The PVT leads to an increase during the summer. For alternative 2, the lows during the winter is quite lower than the other alternatives due to the smaller BHE field and not a sufficient heat injection from the PVT. In addition, the degradation of the temperature over the years is lower for alternative 3, which will lead to better KPIs in the long-run.

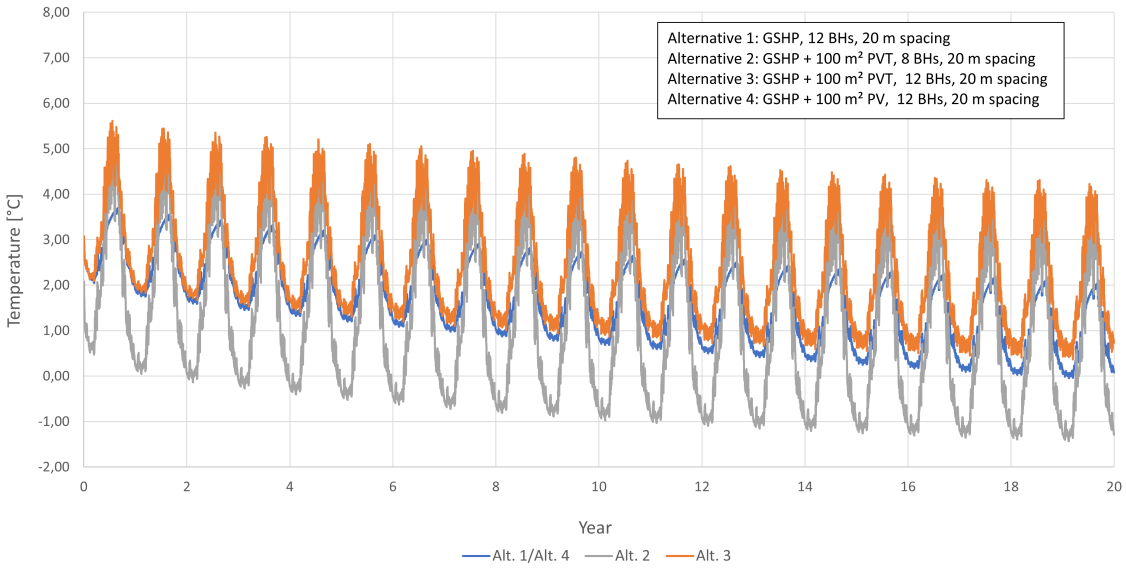


Figure 5.6: Average brine fluid temperature for the alternatives the first 20 years.

# 6 Economical analysis

An important aspect when comparing different energy solution, in addition to performance, is economy. Technical results have shown that PVT improves the performance of a GSHP system, but PVT also comes with a high investment cost that the elevated performance should compensate for.

This section contains a simple economical assessment to compare the three different models presented in this thesis. The goal is to investigate if adding PVT and reducing the size of the BHE field is economically beneficial, and in addition compare it to a system with PV panels instead of PVT. The models being compared are the following:

- Alternative 1: GSHP with 12 BHs
- Alternative 2: GSHP with 8 BHs and 100 $m^2$ PVT
- Alternative 3: GSHP with 12 BHs and 100 $m^2$ PV

The investment criteria and economical principles applied are explained in section 2.9. A summary of the cost and lifetime of the components are listed in table 6.1, and values for economical parameters can be seen in table 6.2. Due to the lifetime of the HP, PV and PVT being 20 years, the time horizon for the analysis is set to 20 years. The lifetime of the BH field is 40-100 years. One could argue that the BHs are permanent and does not have a salvage value. The analysis has however been performed by including the salvage value of the BHs, with an expected lifetime of the wells of 60 and 100 years. According to the supervisor, a discount rate between 4-7% is usually used in cases like this, and it is therefore set to 5.5%. The reference case is electric heating, as this is a conventional heating method in Norway. The surplus electricity production from the PV/PVT is assumed exported back to the grid for the same price as imported energy. It has therefore, as a simplification, been subtracted from the total energy use of the system.

In addition, it is possible to get financial contributions from Enova [56]. Housing associations and businesses can apply for contributions up to 45% of the total investment with a maximum of 1 million NOK. A brine-water HP can give 1 600 NOK/kW and a ST system 201 NOK/$m^2$. This is however not included in this analsysis. The yearly maintenance cost of the heat pump is assumed 1% of the investment cost of it [33].

| Component | Price | Lifetime | Economy and lifetime described in section |
|---|---|---|---|
| PV | $<$ 30 kWp: 1 000 EUR/kWp<br>$>$ 30 kWp: 900 EUR/kWp | 20 years | 2.5.1 |
| PVT | $<$ 30 kWp: 2 400 EUR/kWp<br>$>$ 30 kWp: 2 200 EUR/kWp | 20 years | 2.6.1 |
| HP | 11 000 EUR | 20 years | 2.7.1 |
| BHE | 5 800 EUR/BHE | 40-100 years | 2.7.1 |

Table 6.1: Information used to perform the economical assessment.

| Parameter | Value |
|---|---|
| $r$ | 5.5 % |
| $\varepsilon_{5,20}$ | 0.08368 |
| Time horizon | 20 years |

Table 6.2: Values for economical parameters used.

The results of the analysis with an electricity price of 1.44 NOK/kWh (ca. 0.12 EUR/kWh) are summarized in table 6.3. It can be seen that all alternatives have a lower annual total cost than electric heating, but alternative 2 with PVT has the highest one among the alternatives. The lowest annual cost is achieved for alternative 3 with PV. The efficiency of the PV is higher than the PV efficiency of the PVT, which could make the comparison slightly unfair. However, this does indicate that the reduction of drilling cost is not returned in energy savings by adding PVT to the system. Additionally, all alternatives have a rather short pay-back time, both when you consider a lifetime of 60 and 100 years for the BHE field, that is acceptable considering the components lifetimes. Both the alternative with PV and PVT have a larger annual saving than alternative 1, but due to the high investment cost their pay-back times are longer.

| | Electric heating | Alternative 1 | Alternative 2 | Alternative 3 |
|---|---|---|---|---|
| Energy use [kWh/year] | 221 299 | 80 108 | 63 148 | 60 384 |
| Total investment, 60 years [EUR] | - | 64 697 | 97 198 | 85 697 |
| Total investment, 100 years [EUR] | - | 61 517 | 95 078 | 82 517 |
| Annual total cost, 60 years [EUR/year] | 26 556 | 15 026 | 15 711 | 14 417 |
| Annual total cost, 100 years [EUR/year] | 26 555 | 14 761 | 15 533 | 14 151 |
| Savings [EUR/year] | - | 16 833 | 18 868 | 19 200 |
| Pay-back time, 60 years | - | 4.4 | 6.2 | 5.3 |
| Pay-back time, 100 years | - | 4.2 | 6.1 | 5.0 |

Table 6.3: Results of the economical analysis with an energy price of 0.12 EUR/kWh.

## 6.1 Effect of an increased electricity price

The electricity price is unpredictable and can have substantial changes over a 20 year period. An increased electricity price will make the need for reducing the energy consumption higher, from an economical perspective. Energy efficient systems will have a higher energy saving and the pay-back time is reduced. In a case with a higher electricity price of 2.50 NOK/kWh (ca. 0.21 EUR/kWh), the results of the analysis is as summarized in table 6.4. The pay-off times ranges from approximately 2 to 3 years, which is well within the components' lifetimes. The shortest pay-back time is still achieved with alternative 1, followed by alternative 3, although alternative 2 and 3 both have a lower annual total cost.

An important aspect is that these results are achieved with an annual average electricity price. During the summer months, when the produced energy in the PV/PVT is higher than the consumption of the system, the electricity price is usually lower than the yearly average. By this, the savings from exporting surplus electricity may be lower in reality. This is done for both alternatives so it should not affect the outcome when comparing alternative 2 and 3. But it could have a false positive effect when compared to alternative 1 and electric heating.

| | Electric heating | Alternative 1 | Alternative 2 | Alternative 3 |
|---|---|---|---|---|
| Energy use [kWh] | 221 299 | 80 108 | 63 148 | 60 384 |
| Total investment, 60 years [EUR] | - | 64 697 | 97 198 | 85 697 |
| Total investment, 100 years [EUR] | - | 61 517 | 95 078 | 82 517 |
| Annual total cost, 60 years [EUR/year] | 46 473 | 22 236 | 21 394 | 19 851 |
| Annual total cost, 100 years [EUR/year] | 46 473 | 21 970 | 21 217 | 19 585 |
| Savings [EUR/year] | - | 29 549 | 33 102 | 33 682 |
| Pay-back time, 60 years | - | 2.4 | 3.3 | 2.8 |
| Pay-back time, 100 years | - | 2.3 | 3.2 | 2.7 |

Table 6.4: Results of the economical analysis with an energy price of 0.21 EUR/kWh.

## 6.2 Effect of a decreased electricity price

Another possible scenario is that the electricity price could undergo a diminution. Accordingly, the energy saving measurements will be less profitable. A scenario with a lower energy price of 0.70 NOK/kWh (ca. 0.06 EUR/kWh) can be seen in table 6.5. Under these circumstances, the pay-back time is increased significantly for all cases. Alternative 2 with PVT especially has a high pay-back time with 15 years, but this is still within its lifetime. The difference in annual total cost between electric heating and the alternatives is also markedly reduced.

| | Electric heating | Alternative 1 | Alternative 2 | Alternative 3 |
|---|---|---|---|---|
| Energy use [kWh] | 221 299 | 80 108 | 63 148 | 60 384 |
| Total investment, 60 years [EUR] | - | 64 697 | 97 198 | 85 697 |
| Total investment, 100 years [EUR] | - | 61 517 | 95 078 | 82 517 |
| Annual total cost, 60 years [EUR/year] | 13 278 | 10 220 | 11 922 | 10 794 |
| Annual total cost, 100 years [EUR/year] | 13 278 | 9 954 | 11 745 | 10 528 |
| Savings [EUR/year] | - | 8 361 | 9 379 | 9 544 |
| Pay-back time, 60 years | - | 10.3 | 15.8 | 12.7 |
| Pay-back time, 100 years | - | 9.7 | 15.2 | 12.1 |

Table 6.5: Results of the economical analysis with an energy price of 0.06 EUR/kWh.

# 7 Conclusion

The goal of this work was to analyze the performance of a GSHP with PVT for a typical Norwegian apartment block in TRNSYS in high latitudes, and compare it to a stand-alone GSHP and a GSHP with PV. The emphasis was placed on energy efficiency, but a focus has also been on the thermal behavior of the BHs and reducing the drilling cost.

After varying different parameters for the size of the storage, the results showed that the correct sizing of it is critical. An undersized storage will lead to cold BHs and a larger decrease in the system's performance over the years. Many apartment blocks are built in densely populated areas with a limited space for large BHE fields. By adding PVT, the field can be reduced with fewer BHs or a smaller spacing between them. The results showed that undersizing the BHE field did not provide satisfactory energy and cost efficiency, compared to a conventional sized GSHP system both with and without PV. The most cost efficient systems were the systems consisting of a stand-alone GSHP and a GSHP with 100 $m^2$ of PV. A GSHP system with 100 $m^2$ of PVT gave a payback time within its lifetime, but a higher annual total cost.

The work has shown that adding PVT to a conventional sized BTES system can boost the efficiency and lead to a more stable temperature of the ground. The degradation of the performance over the years is also reduced by adding PVT. Simulations with different sizes of PVT collector area showed that the auxiliary heating for SH is barely reduced with a bigger collector, and increasing the area of it thus has a limited return on the performance of the system. When increasing the power coverage factor of the GSHP, the auxiliary heating for SH was still not reduced with a larger collector.

# 8 Further work

The work has shown that adding 100 $m^2$ of PVT to a GSHP with 8 BHs does not improve the performance and energy savings sufficient to match a GSHP with 12 BHs. A reduction of 4 BHs is a relatively large reduction, and reducing it by less BHs should be studied. In addition, the GSHP system with PV outperforms the PVT with the electricity production and annual total cost. This is likely due to a higher PV efficiency for the PV panel than the PVT, and investigating it with more similar prerequisites would be beneficial, to determine if the removal of heat underneath the PV increases its performance. In addition, a system with PV and ST collectors should be compared to the PVT.

When the power coverage factor of the HP was increased, the electricity consumption during months with a moderate heating load was increased, compared to a lower coverage. This should be further investigated, and looking into using a two-stage HP could possibly improve this.

For distribution of surplus electricity production from the PV and PVT, it is assumed sold for the same price as for imported electricity. This is not necessarily the case, and other cases where it is sold for a lower price could be beneficial to look into.

To make the results even more reliable, some of the simplifications should be removed. The piping and DHW distribution were not included. Circulation in the DHW distribution will contribute with a significant heat loss, and in addition, each floor of the building is constructed as one zone in the simulation models.

The system configurations are barely reaching an SPF4 of 3. This should be further investigated. It could be beneficial to simulate with other control algorithms, especially for SH and DHW.

In the academic analysis, only one discount rate of 5.5 % was used, and possible financial contributions from Enova was not included. Other discount rates and a reduction in investment cost could change which option is the most viable.

# References


[1] Energifakta Norge. *Energibruken i ulike sektorer*. 2017. URL: https://energifaktanorge.no/norsk-energibruk/energibruken-i-ulike-sektorer/#husholdninger (visited on 05/31/2023).

[2] Norsk Varmepumpeforening. *Veksten fortsetter for varmepumper i Norge*. 2017. URL: https://www.novap.no/artikler/artikler-veksten-fortsetter-for-varmepumper-i-norge (visited on 05/31/2023).

[3] A. M. E. Buan. *Analysis of ground-source heat pump and hybrid PVT for Norwegian conditions*. Tech. rep. NTNU, 2022.

[4] Statistics Norway. *Boliger*. 2022. URL: https://www.ssb.no/bygg-bolig-og-eiendom/bolig-og-boforhold/statistikk/boliger (visited on 03/29/2023).

[5] Energi- og vannressursavdelingen (EV). *Energibruk, energiomlegging og effektivisering*. 2021. URL: https://www.regjeringen.no/no/tema/energi/fornybar-energi/energibruk-energiomlegging-og-effektivisering/id2350747/ (visited on 03/29/2023).

[6] *Enovas byggstatistikk 2017*. Tech. rep. Enova SF, 2017.

[7] Statistics Norway. *06266: Boliger, etter region, bygningsår, statistikkvariabel, år og bygningstype*. n.d. URL: https://www.ssb.no/statbank/table/06266/tableViewLayout1/ (visited on 03/29/2023).

[8] Statistics Norway. *Rekordhøy strømpris i 2022 – dempet av strømstøtte*. 2023. URL: https://www.ssb.no/energi-og-industri/energi/statistikk/elektrisitetspriser/artikler/rekordhoy-strompris-i-2022--dempet-av-stromstotte (visited on 05/30/2023).

[9] Fjordkraft. *Vilkår Solkonto*. 2022. URL: https://www.fjordkraft.no/strom/stromavtale/solkraft/vilkar-solkonto/?_gl=1*3059vm*_up*MQ..&gclid=CjwKCAjwvdajBhBEEiwAeMh1U7IeCc3NzAFZwB48WPSg_2hus43dV4pW7frNI3Tem-JunfHNcKm_eBoC1tIQAvD_BwE (visited on 05/30/2023).

[10] U. M. Halvorsen et al. *Mulighetsstudie. Solenergi i Norge*. Tech. rep. https://sintef.brage.unit.no/sintef-xmlui/handle/11250/2427475: Sintef, KanEnergi, 2011.

[11] Norges vassdrags- og energidirektorat. *Solkraft*. 2023. URL: https://www.nve.no/energi/energisystem/solkraft/ (visited on 01/16/2023).

[12] S. Nagarajan, H. Barshilia, and K. Rajam. *Review of sputter deposited mid- to high- temperature solar selective coatings for Flat Plate/Evacuated tube collectors and solar thermal power generation applications*. Dec. 2010.

[13] K. Hudon. "Chapter 20 - Solar Energy – Water Heating". In: *Future Energy (Second Edition)*. Ed. by Trevor M. Letcher. Second Edition. Boston: Elsevier,

2014, pp. 433–451. ISBN: 978-0-08-099424-6. DOI: https://doi.org/10.1016/B978-0-08-099424-6.00020-X. URL: https://www.sciencedirect.com/science/article/pii/B978008099424600020X.

[14] L. Evangelisti, R. De Lieto Vollaro, and F. Asdrubali. "Latest advances on solar thermal collectors: A comprehensive review". In: *Renewable and Sustainable Energy Reviews* 114 (2019), p. 109318. ISSN: 1364-0321. DOI: https://doi.org/10.1016/j.rser.2019.109318. URL: https://www.sciencedirect.com/science/article/pii/S136403211930526X.

[15] S. Mohasseb and A. Kasaeian. "Comparing the Performance of Flat Plate Collector and Evacuated Tube Collector for Building and Industrial Usage in Hot and Cold Climate in Iran with TRNSYS Software". In: Nov. 2014.

[16] Boligsmart. *Hva koster solfanger? Pris i 2023*. n.d. URL: https://www.boligsmart.no/pris/solfanger (visited on 04/27/2023).

[17] Norsk Solenergiforening. *Solfangere*. n.d. URL: https://www.solenergi.no/solvarme (visited on 04/27/2023).

[18] Free Energy. *SOLEN SOM DRIVKRAFT*. n.d. URL: https://www.free-energy.com/solenergi (visited on 10/27/2022).

[19] J. H. Kim and J. T. Kim. "Comparison of electrical and thermal performances of glazed and unglazed PVT collectors". In: *International Journal of Photoenergy* 2012 (2012).

[20] J.H. Kim and J.T. Kim. "The experimental performance of an unglazed PVT collector with two different absorber types". In: *International Journal of Photoenergy* 2012 (2012).

[21] Dualsun. *DualSun SPRING*. n.d. URL: https://dualsun.com/en/products/dualsun-spring/ (visited on 04/27/2023).

[22] S. B. Riffat and E. Cuce. "A review on hybrid photovoltaic/thermal collectors and systems". In: *International Journal of Low-Carbon Technologies* 6.3 (July 2011), pp. 212–241. ISSN: 1748-1317. DOI: 10.1093/ijlct/ctr016. eprint: https://academic.oup.com/ijlct/article-pdf/6/3/212/1986079/ctr016.pdf. URL: https://doi.org/10.1093/ijlct/ctr016.

[23] K. D. Huff. In: *Storage and Hybridization of Nuclear Energy*. Ed. by H. Bindra and S. Revankar. Academic Press, 2019. ISBN: 978-0-12-813975-2. DOI: https://doi.org/10.1016/B978-0-12-813975-2.00001-6. URL: https://www.sciencedirect.com/science/article/pii/B9780128139752000016.

[24] G. Hellström. "Thermal performance of borehold heat exchangers". In: *Stockton International Geothermal Conference: 16/03/1998-17/03/1998*. 1998.

[25] E. Nilsson. *Borehole Thermal Energy Storage Systems for Storage of Industrial Excess Heat: Performance Evaluation and Modelling*. Vol. 1872. Linköping University Electronic Press, 2020.

[26] H. Skarphagen et al. "Design considerations for borehole thermal energy storage (BTES): A review with emphasis on convective heat transfer". In: *Geofluids* 2019 (2019).

[27] Daniel Pahud. "Geothermal energy and heat storage". In: *Cannobio: SUPSI DCT LEEE. Scuola Universitaria Professionale della Svizzera Italiana* (2002).

[28] E. Bertram, J. Glembin, and G. Rockendorf. "Unglazed PVT collectors as additional heat source in heat pump systems with borehole heat exchanger". In: *Energy Procedia* 30 (2012). 1st International Conference on Solar Heating and Coolingfor Buildings and Industry (SHC 2012), pp. 414–423. ISSN: 1876-6102. DOI: https://doi.org/10.1016/j.egypro.2012.11.049. URL: https://www.sciencedirect.com/science/article/pii/S1876610212015652.

[29] E. Bertram. "Solar Assisted Heat Pump Systems with Ground Heat Exchanger – Simulation Studies". In: *Energy Procedia* 48 (2014). Proceedings of the 2nd International Conference on Solar Heating and Cooling for Buildings and Industry (SHC 2013), pp. 505–514. ISSN: 1876-6102. DOI: https://doi.org/10.1016/j.egypro.2014.02.060. URL: https://www.sciencedirect.com/science/article/pii/S1876610214003221.

[30] E. Kjellsson, G. Hellström, and B. Perers. "Optimization of systems with the combination of ground-source heat pump and solar collectors in dwellings". In: *Energy* 35.6 (2010). 7th International Conference on Sustainable Energy Technologies, pp. 2667–2673. ISSN: 0360-5442. DOI: https://doi.org/10.1016/j.energy.2009.04.011. URL: https://www.sciencedirect.com/science/article/pii/S036054420900108X.

[31] B. Nordell and G. Hellström. "High temperature solar heated seasonal storage system for low temperature heating of buildings". In: *Solar Energy* 69 (Dec. 2000), pp. 511–523. DOI: 10.1016/S0038-092X(00)00120-1.

[32] N. Sommerfeldt and H. Madani. "Review of Solar PV/Thermal Plus Ground Source Heat Pump Systems for European Multi-Family Houses". In: Jan. 2016, pp. 1–12. DOI: 10.18086/eurosun.2016.08.15.

[33] R. K. Ramstad. *Grunnvarme i Norge - Kartlegging av økonomisk potensial*. Tech. rep. https://publikasjoner.nve.no/oppdragsrapportA/2011/oppdragsrapportA2011$_0$5.*pdf*: Norges vassdrags- og energidirektorat, 2011.

[34] Varmepumpeportalen. *Dette koster bergvarme? Se oversikt over priser her.* 2023. URL: https://varmepumpeportalen.no/bergvarme-pris (visited on 05/16/2023).

[35] N. Sommerfeldt and H. Madani. *Effsys Expand Final Report - Ground Source Heat Pumps for Swedish Multi-Family Houses: Innovative Co-Generation and Thermal Storage Strategies.* June 2018. DOI: 10.13140/RG.2.2.12514.38084.

[36] P. Sporn and E.R. Ambrose. "The heat pump and solar energy". In: *Proceedings of the world symposium on applied solar energy.* 1955, pp. 1–5.

[37] P. Omojaro and C. Breitkopf. "Direct expansion solar assisted heat pumps: A review of applications and recent research". In: *Renewable and Sustainable Energy Reviews* 22 (2013), pp. 33–45. ISSN: 1364-0321. DOI: https://doi.org/10.1016/j.rser.2013.01.029. URL: https://www.sciencedirect.com/science/article/pii/S1364032113000609.

[38] J. W. Andrews. *EVALUATION OF FLAT-PLATE PHOTOVOLTAIC THERMAL HYBRID SYSTEMS FOR SOLAR ENERGY UTILIZATION.* Tech. rep. BROOKHAVEN NATIONAL LABORATORY (US), 1981.

[39] D. Sauter et al. "Solar Thermal Regeneration of Borehole Heat Exchangers in Urban and Suburban Districts". In: *Journal of Physics: Conference Series.* Vol. 2042. 1. IOP Publishing. 2021, p. 012094.

[40] N. Sommerfeldt and H. Madani. "In-depth techno-economic analysis of PV/Thermal plus ground source heat pump systems for multi-family houses in a heating dominated climate". In: *Solar Energy* 190 (2019), pp. 44–62. ISSN: 0038-092X. DOI: https://doi.org/10.1016/j.solener.2019.07.080. URL: https://www.sciencedirect.com/science/article/pii/S0038092X19307510.

[41] Farzin M Rad, Alan S Fung, and Wey H Leong. "Combined solar thermal and ground source heat pump system". In: *IBPSA* (2009).

[42] Enova. *Rehabilitering av Varden skole i Bergen.* n.d. URL: https://www.enova.no/om-enova/om-organisasjonen/teknologiportefoljen/rehabilitering-av-varden-skole-i-bergen/ (visited on 05/16/2023).

[43] FutureBuilt. *FutureBuilt kvalitetskriterier.* n.d. URL: https://www.futurebuilt.no/FutureBuilt-kvalitetskriterier (visited on 05/16/2023).

[44] Adressavisen. – *Vi er stolte over å være med på Gartnersletta.* n.d. URL: https://www.adressa.no/brandStudio/feature/v/skanska/vi-er-stolte-over-a-vaere-med-pa-gartnersletta/ (visited on 06/08/2023).

[45] Skanska. *Pilotprojekt på vägen mot klimatneutralt Skanska.* n.d. URL: https://www.skanska.se/vart-erbjudande/vara-projekt/250260/Bla-Port%5C%2C-Karlskrona (visited on 05/17/2023).

[46] H. H. Faanes et al. *Compendium: TET4135 Energy Systems Planning and Operation*. 2016. URL: https://ntnu.blackboard.com (visited on 05/22/2023).

[47] NTNU and SINTEF. *ENØK i bygninger: effektiv energibruk*. Norge: Gyldendal undervisning, 2007.

[48] Norsk Standard. *SN-NSPEK 3031:2020 Bygningers energiytelse — Beregning av energibehov og energiforsyning*. 2020. URL: https://www.standard.no/no/Nettbutikk/produktkatalogen/Produktpresentasjon/?ProductID=1124340 (visited on 09/25/2022).

[49] J. Calisti, T. Loga, and B. Stein. *TABULA WebTool*. Sept. 30, 2022. URL: https://webtool.building-typology.eu/#bm.

[50] TESS. *TESS COMPONENT LIBRARIES - General Descriptions*. n.d. URL: http://www.trnsys.com/tess-libraries/TESSLibs17_General_Descriptions.pdf (visited on 01/20/2023).

[51] J.W. Thornton et al. *TESSLibs 17 - GHP Library Mathematical Reference*. Madison, 2005.

[52] DualSun. *FLASH 425 Shingle Black*. 2023. URL: https://dualsun.com/wp-content/uploads/dualsun-en-datasheet-flash-425-shingle-black.pdf (visited on 05/17/2023).

[53] J.W. Thornton et al. *TESSLibs 17 - Electrical Library Mathematical Reference*. Madison, 2005.

[54] S.J. Rees. In: *Advances in Ground-Source Heat Pump Systems*. Ed. by S. J. Rees. Woodhead Publishing, 2016. ISBN: 978-0-08-100311-4.

[55] M. Burkhalter and Y. Felder. "Analysis of solar-assisted heat pump using hybrid PVT in Norwegian conditions". Norwegian University of Science and Technology, 2022.

[56] Enova. *Varmesentraler*. n.d. URL: https://www.enova.no/bedrift/bygg-og-eiendom/varmesentraler/ (visited on 04/27/2023).

# A Models in TRNSYS

## A.1 Model 1

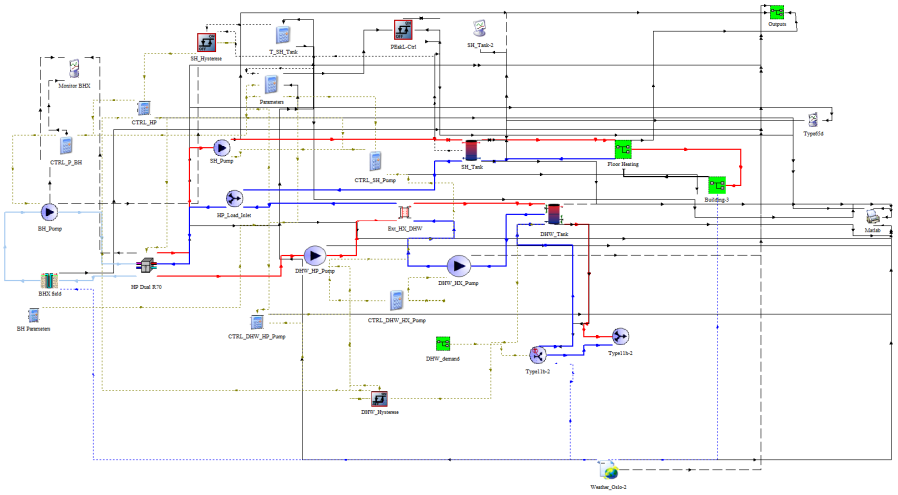

Figure A.1: TRNSYS model of the base case.

## A.2 Model 2

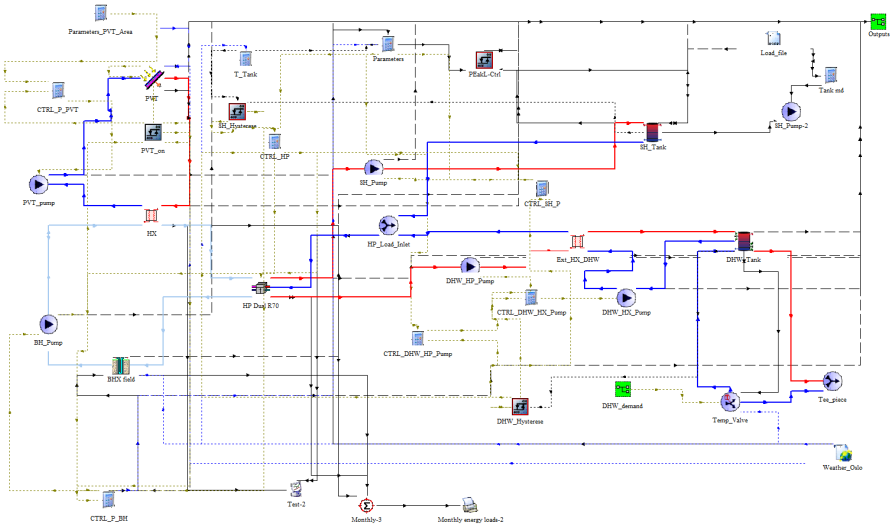

Figure A.2: TRNSYS model of the GSHP with PVT.

# B Other results, GSHP + PVT

## B.1 Spacing of 20 m

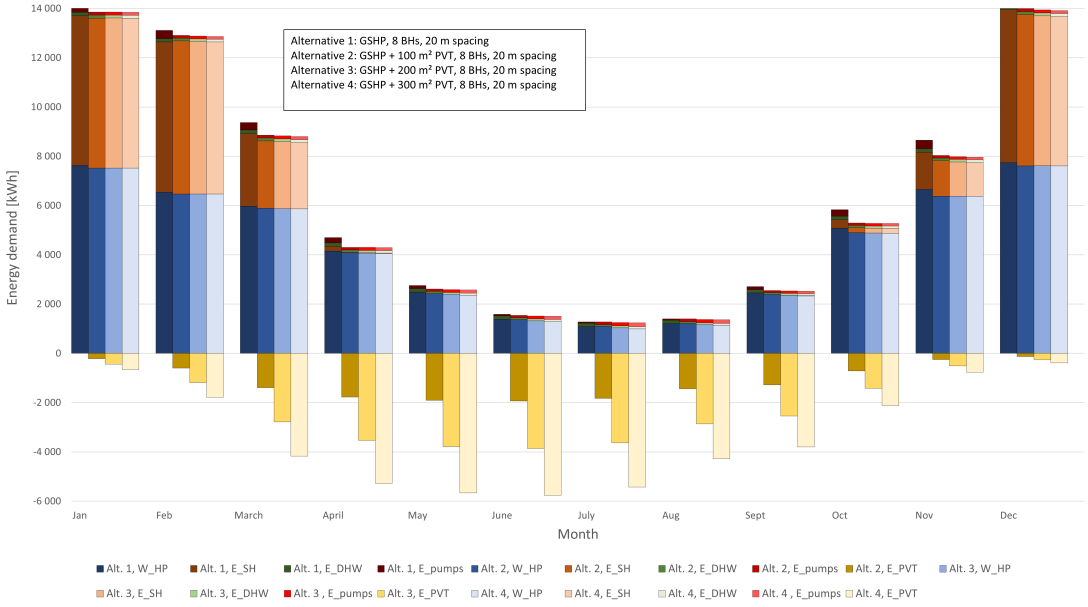


Figure B.1: Comparison of the energy consumption with regards to the area of PVT with 8 BHs in case 1.

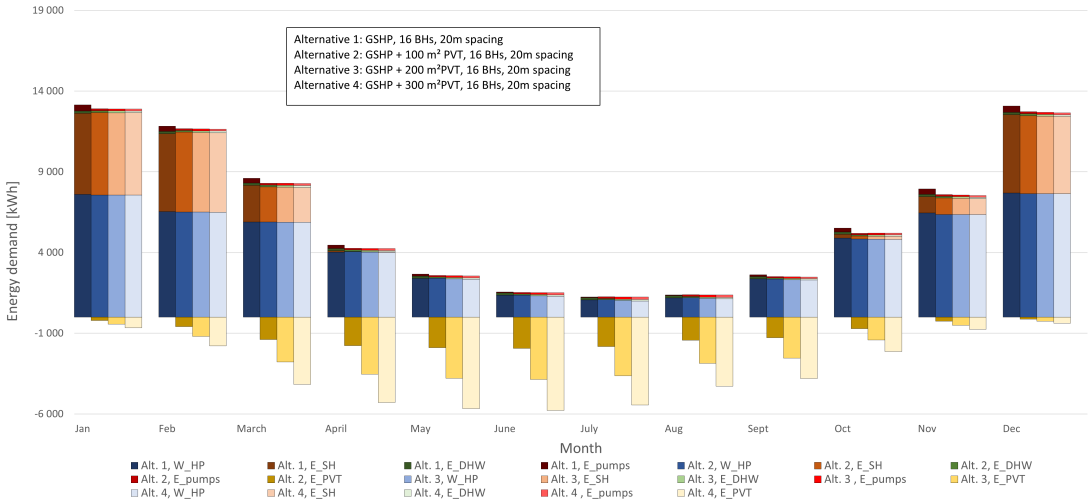


Figure B.2: Comparison of the energy consumption with regards to the area of PVT with 16 BHs in case 1.

| PVT collector area [m$^2$] | Number of boreholes | Year | SPF [-] | SPF4 [-] | $Reg_{frac}$ [-] | Minimum $T_m$ [° C] |
|---|---|---|---|---|---|---|
| 50 | 8 | 1 | 3.70 | 2.75 | 0.09 | 0.20 |
| | | 50 | 3.47 | 2.48 | 0.12 | -2.46 |
| | 12 | 1 | 3.83 | 2.91 | 0.08 | 1.97 |
| | | 50 | 3.61 | 2.64 | 0.11 | -0.72 |
| | 16 | 1 | 3.88 | 2.98 | 0.08 | 2.64 |
| | | 50 | 3.69 | 2.74 | 0.11 | 0.15 |
| 100 | 8 | 1 | 3.72 | 2.76 | 0.17 | 0.25 |
| | | 50 | 3.52 | 2.52 | 0.22 | -2.10 |
| | 12 | 1 | 3.84 | 2.92 | 0.16 | 2.01 |
| | | 50 | 3.65 | 2.68 | 0.21 | -0.39 |
| | 16 | 1 | 3.89 | 2.99 | 0.16 | 2.68 |
| | | 50 | 3.73 | 2.77 | 0.20 | 0.42 |
| 150 | 8 | 1 | 3.74 | 2.77 | 0.24 | 0.30 |
| | | 50 | 3.56 | 2.56 | 0.31 | -1.78 |
| | 12 | 1 | 3.86 | 2.92 | 0.23 | 2.05 |
| | | 50 | 3.69 | 2.71 | 0.30 | -0.10 |
| | 16 | 1 | 3.91 | 2.99 | 0.23 | 2.73 |
| | | 50 | 3.77 | 2.81 | 0.29 | 0.66 |

Table B.1: Summary of the KPIs for the GSHP PVT over 50 years with a brine fluid specific heat capacity of 4.19 $kJ/(K \cdot kg)$.

## B.2 Spacing of 10 m

| PVT collector area [m$^2$] | Number of boreholes | Year | SPF [-] | SPF4 [-] | $Reg_{frac}$ [-] | Minimum $T_m$ [° C] |
|---|---|---|---|---|---|---|
| 50 | 8 | 1 | 3.69 | 2.74 | 0.09 | -0.04 |
| | | 50 | 3.37 | 2.39 | 0.14 | -3.57 |
| | 12 | 1 | 3.82 | 2.90 | 0.09 | 1.76 |
| | | 50 | 3.50 | 2.52 | 0.13 | -2.06 |
| | 16 | 1 | 3.88 | 2.98 | 0.08 | 2.44 |
| | | 50 | 3.58 | 2.61 | 0.13 | -1.26 |
| 100 | 8 | 1 | 3.72 | 2.75 | 0.17 | 0.05 |
| | | 50 | 3.44 | 2.44 | 0.25 | -3.01 |
| | 12 | 1 | 3.84 | 2.91 | 0.16 | 1.86 |
| | | 50 | 3.56 | 2.58 | 0.24 | -1.53 |
| | 16 | 1 | 3.89 | 2.98 | 0.16 | 2.51 |
| | | 50 | 3.63 | 2.67 | 0.23 | -0.79 |
| 150 | 8 | 1 | 3.73 | 2.76 | 0.26 | 0.14 |
| | | 50 | 3.50 | 2.49 | 0.34 | -2.53 |
| | 12 | 1 | 3.85 | 2.92 | 0.24 | 1.94 |
| | | 50 | 3.62 | 2.63 | 0.33 | -1.06 |
| | 16 | 1 | 3.90 | 2.99 | 0.24 | 2.57 |
| | | 50 | 3.68 | 2.71 | 0.32 | -0.37 |

Table B.2: Summary of the KPIs for the GSHP with PVT over 50 years with a brine fluid specific heat capacity of 4.19 $kJ/(K \cdot kg)$.

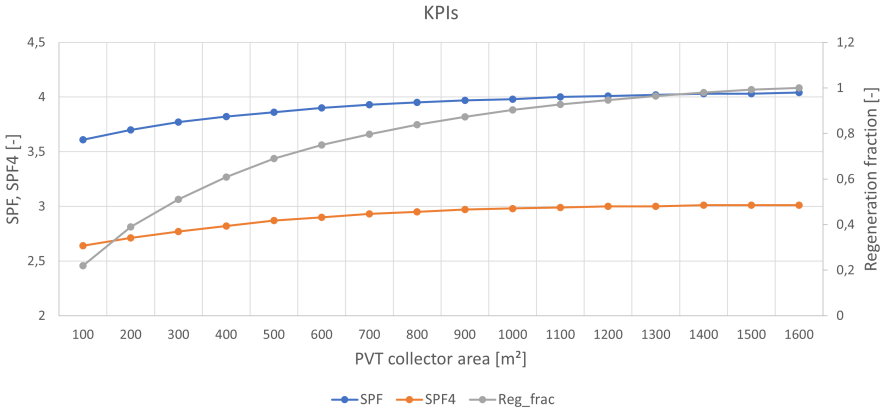


Figure B.3: KPIs for the system with different sizes of PVT collector with a brine fluid specific heat capacity of 4.19 $kJ/(K \cdot kg)$.

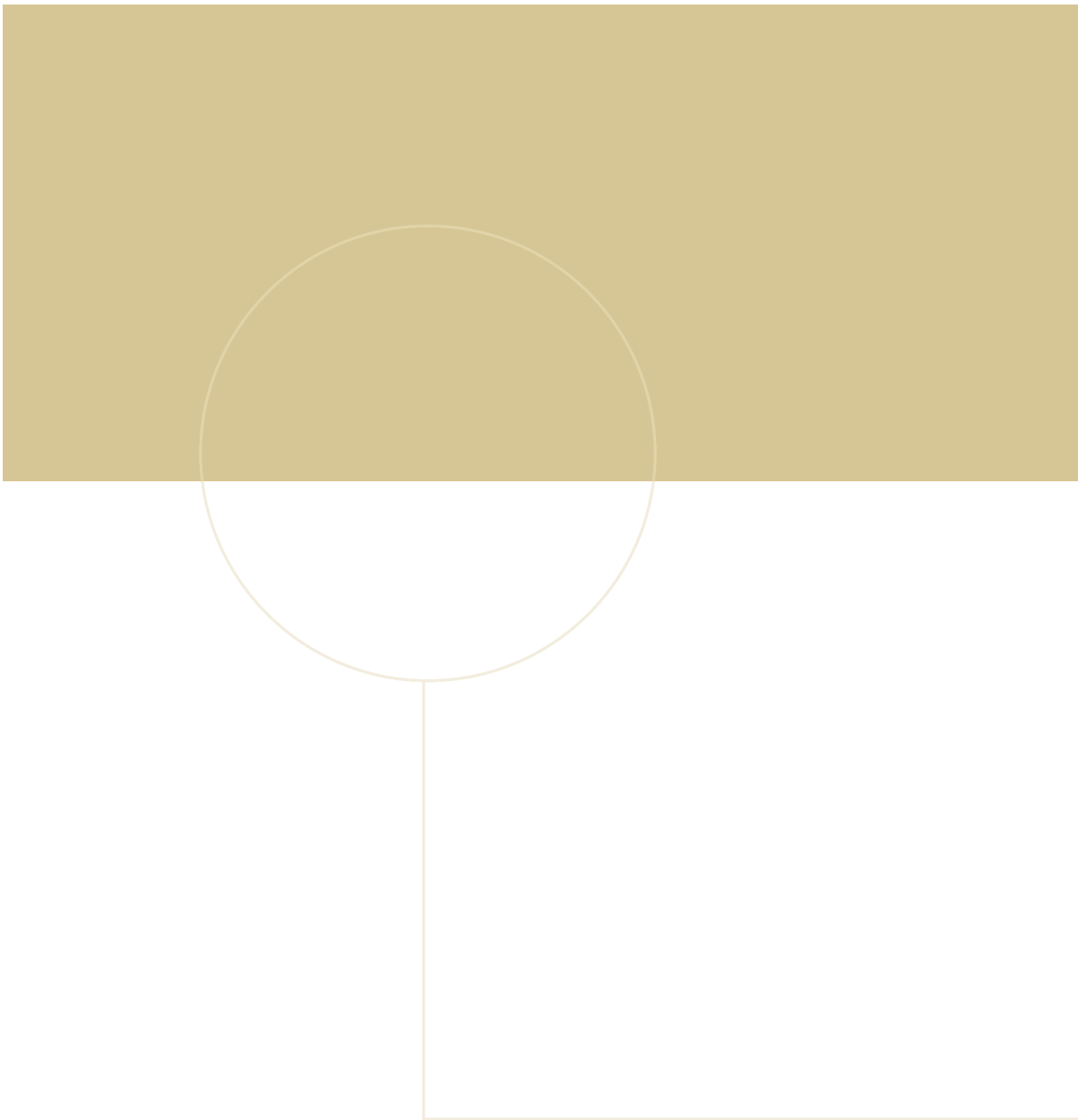

NTNU

Norwegian University of
Science and Technology